The Geological Society of America Bulletin

Potential K-Pg tsunami deposits in the intra-Tethyan Adriatic carbonate platform section of Hvar (Croatia)

--Manuscript Draft--

Manuscript Number:	B31084R4
Full Title:	Potential K-Pg tsunami deposits in the intra-Tethyan Adriatic carbonate platform section of Hvar (Croatia)
Short Title:	K-Pg tsunami in the Tethys?
Article Type:	Article
Keywords:	Cretaceous-Paleogene event, tsunami, Adriatic carbonate platform, western Tethys.
Corresponding Author:	Tvrtko Korbar, Ph.D. Croatian Geological Survey Zagreb, CROATIA
Corresponding Author's Institution:	Croatian Geological Survey
First Author:	Tvrtko Korbar, Ph.D.
Order of Authors:	Tvrtko Korbar, Ph.D.
	Alessandro Montanari, PhD
	Vlasta Premec Fuček, PhD
	Ladislav Fuček
	Rodolfo Coccioni, PhD
	Iain Mc Donald, PhD
	Philippe Claeys, PhD
	Toni Schulz, PhD
	Christian Koeberl, PhD
Abstract:	An exceptional 47-m-thick succession of Maastrichtian to Paleocene inner-platform carbonates is exposed in the Dalmatian island of Hvar (Adriatic Sea, Croatia) in a seaside locality called Majerovica. The middle part of this succession comprises a ~5 m thick intraformational massive deposit, which is underlain by well-bedded peritidal inner-platform limestones containing latest Maastrichtian rudists and shallow water benthic foraminifera. This deposit includes a polygenic, matrix-supported carbonate breccia characterized by ripped-up platform limestone lithoclasts, up to boulder sized, and polygenic microbreccia in a muddy matrix. The microbreccia contains rare small intraclasts of pelagic mudstone containing terminal Maastrichtian planktonic foraminifera. The deposit is overlain in turn by mudstone containing a planktonic foraminiferal association belonging to the P0 and P Zones of the basal Paleogene, and by shallow-water muddy limestones containing planktonic foraminifera belonging to the P1 Zone. While facies suggest that the deposit was emplaced over the inner platform by a single large tsunami, the biostratigraphic assessment of this section and the presence of enhanced concentrations of platinum group elements, such as iridium in the topmost part of the massive deposit, lend support to the hypothesis that this tsunamite is related to the K-Pg event, triggered by the Chicxulub impact in Yucatán. This is potentially the first case of a tropical carbonate platform sedimentary succession recording the K-Pg event, which provides a new constraint for modeling both the western Tethyan paleogeography and the catastrophic aftermaths of the Chixculub impact at the Cretaceous-Paleogene boundary.
Suggested Reviewers:	
Opposed Reviewers:	
Response to Reviewers:	Dear Editors,

We would like to thank the Associate Editor, Brian Pratt, for his very useful additional suggestions, which helped us to improve the manuscript. We took into account all the comments and suggestions of the AE, as briefly discussed below.

RESPONSE TO COMMENTS OF THE AE:

We have reorganized the Discussion and Conclusion chapter, and left just the “Results” in a separate section.

New Discussion chapter is reorganized into sections according to a more logical order.

We discussed in more details possible alternative interpretations, especially tsunami vs strom mechanism, and highlight the relevance of the depositional setting for the interpretation. Considering that issue, we would like to note that the underlying and overlaying succession (as shown on Fig. 2B and discussed in the text), but also the lateral outcrops of the Sumartin Formation on Hvar (it is not possible to provide a reference to these data, as these are personal observations in the field by the first author), lack any extraordinary flow deposit that could be interpreted as tsunamite or tempestite within this very inner-platform environment. We did not discuss a possible shaking origin of the breccia, as we do not think that such a mechanism was responsible, because of the presence of various lithotypes and size of the lithoclasts in the breccia (including unusual pelagic microintraclasts in the bottom), and an erosion of the underlying sediments, as well as a lack of soft sediment deformation of the underlying microbial laminites.

We replaced some peculiar terms by more common ones, as suggested.

We added several references of some other (the most important) K-Pg sections in the region, along with the latest paper updating the western Mediterranean paleogeography.

The starting explanation of the tsunami origin is now endogenic. However, although the tectonism of course didn't stop during K-Pg boundary time, there was probably a quiescent period, as recorded within the well-constrained pelagic successions in the Adriatic region (i.e., Marche-Umbrian basin).

Considering the AE’s comment regarding the western Mediterranean latest Cretaceous plate configuration, we would like to highlight that according to the updated geotectonic reconstructions, the western Mediterranean has been open for the potential tsunami propagation, in contrast to what was suggested by some previous models. Therefore, the adopted latest Cretaceous plate configuration supports a suggested model of the transatlantic tsunami. However, according to our knowledge, there are no published reports on any section recording K-Pg boundary in shallow-water setting facing the western Tethys. Thus, any possible signature in other localities cannot be evaluated, but we hope that our paper would stimulate similar investigations at other locations.

In the revised text, the Conclusion section comprises just a few the most important issues of the research.

We hope that we were able to successfully answer the remaining open questions, as all the other suggestions of the AE were included in the revised text. The revised version of our ms (text and the updated Figs. 1 and 3, and Table 1) is submitted on the GSAB online system. All the changes can be followed in the Track Changes text file uploaded also to the online system.

On behalf of all the co-authors
Sincerely,
Dr. Tvrtko Korbar
Croatian Geological Survey
Sachsova 2
HR-10000 Zagreb, CROATIA
tvrtko.korbar@hgi-cgs.hr
tel. 00385-1-6160-709
fax. 00385-1-6160-799

RUNNING TITLE: K–Pg tsunami in the Tethys?

Potential K–Pg tsunami deposits in the intra-Tethyan Adriatic carbonate platform section of Hvar (Croatia)

Tvrtko Korbar[1], Alessandro Montanari[2], Vlasta Premec Fućek[3], Ladislav Fuček[1], Rodolfo Coccioni[4], Iain McDonald[5], Philippe Claeys[6], Toni Schulz[7], and Christian Koeberl[7, 8]

[1] Department of Geology, Croatian Geological Survey, Sachsova 2, HR-10000 Zagreb, Croatia.
[2] Osservatorio Geologico di Coldigioco, Cda. Coldigioco 4, 62021 Apiro, Italy.
[3] INA-Industrija Nafte d.d., Exploration and Production BD, Research Laboratory Department, Lovinčićeva 4, 10 000 Zagreb, Croatia.
[4] Istituto di Geologia e Centro di Geobiologia, Università degli Studi di Urbino "Carlo Bo", Campus Scientifico, Località Crocicchia, 61029 Urbino, Italy.
[5] School of Earth, Ocean and Planetary Sciences, Cardiff University, Park Place, Cardiff CF10 3AT, United Kindom.
[6] Department of Earth System Science, DGLG-WE, Vrije Universiteit Brussels Pleinlaan 2, B-1050 Brussels, Belgium.
[7] Department of Lithospheric Research, Center for Earth Sciences, University of Vienna, Althanstrasse 14, A-1090 Vienna, Austria.
[8] Natural History Museum, Burgring 7, A-1010 Vienna, Austria.

Keywords: Cretaceous-Paleogene event, tsunami, Adriatic carbonate platform, western Tethys.

ABSTRACT

An exceptional 47-m-thick succession of Maastrichtian to Paleocene inner-platform carbonates is exposed in the Dalmatian island of Hvar (Adriatic Sea, Croatia) in a seaside locality called Majerovica. The middle part of this succession comprises a ~5 m thick intraformational massive deposit, which is underlain by well-bedded peritidal inner-platform limestones containing latest Maastrichtian rudists and shallow water benthic foraminifera. This deposit includes a polygenic, matrix-supported carbonate breccia characterized by ripped-up platform limestone lithoclasts, up to boulder sized, and polygenic microbreccia in a muddy matrix. The microbreccia contains rare small intraclasts of pelagic mudstone containing terminal Maastrichtian planktonic foraminifera. The deposit is overlain in turn by mudstone containing a planktonic foraminiferal association belonging to the P0 and Pα Zones of the basal Paleogene, and by shallow-water muddy limestones containing planktonic foraminifera belonging to the P1 Zone. While facies suggest that the deposit was emplaced over the inner platform by a single large tsunami, the biostratigraphic assessment of this section and the presence of enhanced concentrations of platinum group elements, such as iridium in the topmost part of the massive deposit, lend support to the hypothesis that this tsunamite is related to the K–Pg event, triggered by the Chicxulub impact in Yucatán. This is potentially the first case of a tropical carbonate platform sedimentary succession recording the K–Pg event, which provides a new constraint for modeling both the western Tethyan paleogeography and the

catastrophic aftermaths of the Chixculub impact at the Cretaceous–Paleogene boundary.

INTRODUCTION

The giant Chicxulub impact in the Yucatán Peninsula of Mexico, which triggered a global mass extinction and extraordinary sedimentary perturbations around the Gulf of Mexico region at the Cretaceous–Paleogene (K–Pg) boundary some 66 million years ago (Renne et al., 2013), is probably the most debated global catastrophic event in Earth's history (e.g., Schulte et al., 2010). The event caused the complete extinction of the dinosaurs, non-turtle marine reptiles, ammonites, and the shallow-water rudists, as well as almost all calcareous nannoplankton and planktonic foraminifera, among which only four dwarf foraminiferal species survived the catastrophe (e.g., Smit, 1982; Olsson et al., 1999; Huber et al., 2002; Arenillas et al., 2006). In continuous deep-marine sections, the K–Pg boundary is also marked by a thin horizon containing anomalous concentrations of platinum group elements (PGE), along with shocked mineral grains and impact-derived spherules from the impact fallout (e.g., Smit and Hertogen, 1980; Alvarez et al., 1980; Alvarez et al., 1990; Alvarez et al., 1995; Claeys et al., 2002; Montanari and Koeberl, 2000; Goderis et al., 2013).

Evidence for major sedimentary perturbations directly related to the impact are reported from the impact site and the surrounding basins of the Gulf of Mexico and Caribbean regions (Bralower et al., 1998), while disturbances such as slumps, slope failures, and related tsunami and/or turbidite deposits have been identified in a few proximal deep-marine facies in the Atlantic domain (Klaus et al. 2000; Norris et al., 2000; Norris and Firth, 2002; Claeys et al., 2002). Considering a relatively enclosed end-Cretaceous central Atlantic basin and distance from the impact site, significant sedimentary perturbations are not expected in more distal basins. A limiting factor is probably attenuation of intensity of earthquakes and/or tsunami(s) triggered by the impact (Bralower et al., 1998; Norris and Firth, 2002). However, it must be pointed out that a detailed record of the K–Pg event is not preserved in shallow-water carbonate platform environments situated on the predictable trajectory of tsunami(s), although it is intuitive that the impact must have severely affected these environments causing the extinction of many benthic taxa (e.g., Vecsei and Moussavian, 1997; Norris et al., 2001; Steuber et al., 2002).

In areas immediately surrounding the 180-km-diameter Chicxulub structure, carbonate platforms were likely destroyed by the earthquake and the gigantic tsunami generated by the impact. For example, the Cuban platform, which was located some 800 km east of Chicxulub in Late Cretaceous time (Dercourt et al., 1993), was buried under a 500-m-thick breccia known as Cacarajicara Formation (Kiyokawa et al., 2002). Globally, many tropical carbonate platform-building organisms were probably killed in the immediate aftermath of the impact due to the abrupt and drastic short-term climate change caused by the impact (Schulte et al., 2010; Vellekoop et al., 2014). Nonetheless, even though they record a complex and sensitive ecosystem, carbonate platforms in the Tethyan realm did survive the K–Pg boundary crisis (Schlüter et al., 2008).

Cretaceous–Paleogene carbonate platform successions in the peri-Adriatic region exhibit a more or less extended hiatus which includes the K–Pg boundary (e.g., Eberli et al., 1993; Bosellini et al., 1999). The Adriatic–Dinaric carbonate platform domain (Fig. 1) was mostly emergent during the latest Cretaceous because of a regional tectonic phase, although in some areas of the Adriatic carbonate platform *sensu stricto*, shallow-water sedimentation, interrupted by periods of subaerial exposure, lasted until the Paleocene (Drobne et al., 1989; Korbar, 2009). A short K–Pg hiatus is present locally in the Karst plateau (Slovenia) and the northwestern part of the platform, areas hitherto considered to be complete (Ogorelec et al., 2007). A succession of the uppermost Maastrichtian and possibly younger inner-platform carbonates is reported also from the island of Brač (Gušić and Jelaska, 1990; Steuber et al., 2005), although there is no biostratigraphic evidence for a Paleocene age of the topmost part of the succession, nor any obvious sedimentary record of the impact event.

In this paper, we present results of an integrated sedimentological, biostratigraphic, and geochemical study of a new section through the Adriatic carbonate platform spanning the K–Pg boundary, situated on the island of Hvar (Croatia). We focus on the middle part of the succession that is characterized by an anomalous massive intraformational deposit and records the last appearances of Cretaceous fossils.

GEOLOGICAL SETTING

The K–Pg Majerovica section in the island of Hvar of the Dalmatian archipelago (Adriatic Sea, Croatia, Figs. 1A and 1B), is located in the central part of the broader peri-Adriatic area, which was part of a microplate of African continental crust, the so-called Adriatic Promontory or Adria (Channell et al., 1979). This north-pointing Mesozoic promontory was in many ways similar to the present day south-pointing promontory of North America, which forms Florida and the Bahamas (D'Argenio, 1970). With the inception of the Pangea breakup at the end of the Permian, and consequent divergence between Africa and Europe, Adria entered in a long lasting passive margin phase of extension, crustal thinning, and consequent subsidence, leading to the formation of epeiric marine basins such as the Umbria-Marche, the Adriatic, and the Lagonegro-Molise basins, and the opening of a small Ligurian Ocean, which represented the westernmost extension of the Tethys Ocean separating this African promontory from the southern European continent (Fig. 1C). In this evolving paleotectonic scenario, extensive Bahamas-type carbonate banks developed (i.e., Abruzzo, Apulia, Adriatic, and Dinaric, along with a few smaller satellite platforms), with the maximum development in the Cretaceous Period. Starting in the late Cretaceous, the switch to a convergence between Africa and Europe and consequent reversal of the regional tectonic regime from extensional to compressional, lead to the Alpine orogenic phase of the Adriatic region and the building of peri-Adriatic fold-and-thrust belts, such as the Apennines, the Southern Alps, and the Dinarides (Fig. 1A).

The Adriatic carbonate platform (ACP) is characterized by a succession of Jurassic to Paleocene carbonates several kilometers thick (Zappaterra, 1994; Vlahović et al., 2005). The Cretaceous succession is normally interrupted by a K–Pg regional unconformity (Vlahović et al., 2005), which is overlain by a Paleocene (Drobne et al., 1989) or Eocene succession of brackish-water limestones (the Kozina beds) and/or an open ramp Foraminiferal Limestones unit passing upward to a siliciclastic flysch (Ćosović et al., 2004). Such a sedimentary succession reflects the development of the Alpine orogenic deformations in the Adriatic region, when the platform was progressively deformed from the NE, and ultimately incorporated into the External Dinarides fold-and-thrust belt. As a consequence of that, the SW part of the ACP is mostly buried under thick Tertiary sediments deposited within the Adriatic foreland

(Korbar, 2009).

The Majerovica section at Hvar represents a fortuitous case in the whole ACP, where a 30-m-thick succession of biostratigraphically defined basal Paleocene limestones rest on top of latest Maastrichtian inner-platform limestones. These strata were spared by the Paleocene-Eocene erosional unconformity which arose as a consequence of a major subaerial exposure, and is characterized by paleokarst and pedogenic features (Brlek et al., 2014; Korbar, 2009).

MATERIAL AND METHODS

The Majerovica section is well exposed along the rocky shoreline of Hvar, stretching below the pedestrian path along the western coast of the Majerovica Cove in the western outskirts of the town of Hvar (43°10'21.73" N - 16°25'41.45" E; detailed location map in Korbar et al., 2010). The section was logged and analyzed in the field and samples were collected for petrographic, micropaleontological, and geochemical analyses. Standard thin sections were used for petrographic and micropaleontological assessments, following–the species concepts summarized by Olsson et al. (1999) and Huber and Leckie (2011), and the CHRONOS online Mesozoic taxonomic dictionary (http://portal.chronos.org), as well as the planktonic foraminiferal biozonation model of Berggren and Pearson (2005) and Wade et al. (2011). For each sample, two or more thin sections were analyzed. Later, samples were taken at closely spaced intervals between 20.30 m and 20.80 m, and more than 80 thin sections were prepared for further study of planktonic index-species. Unfortunately, cold acetolysis treatment following the method of Lirer (2000) proved not to be effective in separating these rare and very small foraminiferal tests from the strongly cemented micritic matrix.

Samples of primary low-Mg calcite were obtained from the outer layers of requeniid rudist valves (three valves per level) collected at two horizons at 2 m and 13 m. These were analyzed for Sr, Mg, Fe, Mn, and for Sr-isotope ratios (Table 1), at Ruhr University (Bochum, Germany), following the method described by Steuber et al. (2005).

A suite of nine samples covering the interval between 15.35 m and 25.60 m were analyzed for the contents of the PGEs and gold at Cardiff University (UK) using nickel sulfide fire assay followed by Te coprecipitation and inductively coupled plasma mass spectrometry (ICP-MS). The full methodology is outlined in Huber et al. (2001) and McDonald and Viljoen (2006). A summary of the PGE concentrations in the unknown samples (samples were analyzed in a blindfold test mode) and the certified reference materials (WITS-1, TDB1 and WPR1) are given in Table 2.

Eight of these samples were analyzed, also in a blindfold test mode, at the University of Vienna (Austria) for $^{187}Os/^{188}Os$ ratios and isotope dilution generated Os and Re concentrations. For this analysis the samples were broken into centimeter-sized chips with an agate mortar and pestle before grinding into a fine powder using a ceramic alumina shatterbox. About 0.5 g of each sample was spiked with a mixed ^{185}Re-^{190}Os tracer before successive addition of inverse aqua regia until the reaction came to an end. The sample aliquots were then treated in an Anton Paar HP-Asher at 100 bars and 170°C over night. Osmium was purified using a carbon tetrachloride solvent extraction technique (Cohen and Waters, 1996), back extracted into concentrated HBr followed by microdistillation (Birck et al., 1997). The samples were finally loaded in HBr for measurement on baked 99.99% Materion Pt filaments and covered with a $Ba(OH)_2$-NaOH activator solution. Osmium isotope ratios were measured as OsO_3^- using thermal ionization mass spectrometry at the Department of Lithospheric Research at the University Vienna using a Finnigan Triton. Signals were detected with an scanning electron microscope in pulse counting mode. All measured ratios were corrected for interferences from isobaric ReO_3^- and OsO_3^- molecules (Re corrections were negligible in most cases). Oxide corrected ratios were mass fractionation corrected to a $^{192}Os/^{188}Os$ ratio of 3.08271 (Shirey and Walker, 1998) using an exponential correction law. A DROsS Os reference solution was measured along with every batch of samples analyzed. Measurements over the course of several months yielded 0.1609 for the $^{187}Os/^{188}Os$ ratio at intensities of up to 50000 counts on ^{192}Os. Total procedural blanks for Os averaged at 0.3 ± 0.2 pg with an $^{187}Os/^{188}Os$ ratio of 0.22. The aqua regia fraction with the remaining Re was dried down, redissolved and chromatographically separated on columns loaded with 2ml AG 1x8 anion exchange resin (100-200 mesh). Rhenium isotope ratios were measured by inductively coupled plasma mass spectrometry at the University Bonn (Germany). Rhenium blanks averaged at 4 ± 3 pg. Measurements of the certified reference material TDB1 yielded a value of 0.615 (6) for the $^{187}Os/^{188}Os$ ratio, 0.76 ppb Re and 0.098 ppb Os, in agreement with literature data (Table 2).

RESULTS

Lithostratigraphy, chronostratigraphy, and sedimentary facies

The lower part of the 47.5 m thick Majerovica section (Fig. 2) is characterized by typical peritidal inner-platform carbonates of the Sumartin Formation (Gušić and Jelaska, 1990; Steuber et al., 2005), which crop out also in the town of Hvar (Korbar et al., 2010). This upper part of Sumartin Formation is predominantly made up of locally dolomitized peritidal limestones: mostly fenestral mudstones, microbial laminites, skeletal wackestone-packstone with ostracodes and miliolids, and floatstones containing late Maastrichtian requieniid rudists, rare radiolitids (*Bournonia adriatica*), and benthonic foraminifera (miliolids, rotaliids, and *Rhapydionina liburnica*; Fig. 4A). Mean $^{87}Sr/^{86}Sr$ values of 0.7078450 and 0.7078446 from the requieniid rudists (Table 1) indicate a terminal Maastrichtian age of this part of the section according to the numerical strontium isotope time scales of Howarth and McArthur (1997) and McArthur et al. (2001).

The most noticeable atypical sedimentological feature in the middle part of the Majerovica section is a ~5 m thick, massive, polygenic, matrix-supported, lithoclastic carbonate breccia, which fill at least 0.5 m deep channels, displaying a distinct erosional contact with underlying reddish microbial laminites and ostracode wackestones (Figs. 2B, 3A, 3B, and 4B). The breccia consists mostly of unsorted, predominantly 1-3 cm long lithoclasts, including ripped-up boulders of the directly underlying and eroded limestones, along with various bioclastic floatstones containing radiolitid and requieniid rudists. The clasts are characterized by plastic deformation and diffused margins. The matrix is polygenic microbreccia characterized by chaotically mixed lime mud, peloidal silt and millimeter- to centimeter-sized bioclasts including miliolids, mollusk fragments, and benthonic foraminifera (Fig. 4C). There are also clasts of various limestone types including rare small fragments of pelagic mudstones containing Maastrichtian planktonic foraminifera (Fig. 4D). It is not easy to distinguish between the matrix of this deposit and the clasts, since it is a mixture of comminuted and partially recrystallized skeletal-bioclastic-peloidal-intraclastic wackestones (Fig. 4E), packstones, grainstones, and floatstones. The same breccia horizon is found at two coastal outcrops laterally, ~200 m west and east (Fig. 3C) from the section, respectively, but further logging and mapping is not possible since the area is covered either by sea or by artificial objects. Thus, it is inferred that the breccia has a lateral extent of at least 400 m.

The uneven upper surface of the massive deposit is overlain by 0.3–1.0 m thick, fine-grained, microbioclastic-peloidal-intraclastic packstone-grainstone, containing small miliolids and ostracodes. This limestone includes intercalations of laterally discontinuous lenticular or abruptly truncated laminae of wackestones containing small planktonic foraminifera (Fig. 4F). Rare, up to 5 cm long mollusk bioclasts and clasts of various limestone types are found sparsely within the deposit (Fig. 3E). The uppermost part of the deposit (at 20.30 m) is characterized by a ~2 cm thick, red-stained horizon of microbioclastic and intraclastic wackestone (Figs. 3E and 3F) containing Maastrichtian planktonic foraminifera, intercalated by irregularly undulating laminoid calcite-filled fenestrae (Fig. 4G). This red-stained horizon is immediately overlain by a ~20 cm thick mudstone layer (Fig. 4G), which contains rare dwarf globigerinids typical of the basal Paleocene (see next section). Above this is a package a few meters thick made up of bioturbated mudstone-wackestone and intraclastic breccia in the lower part, and mudstone-wackestone beds above. These contain rare ostracodes, tiny miliolid and discorbid benthonic foraminifera (Fig. 4H), very rare characean calcareous algae, and planktonic foraminifera typical of the lowermost Paleocene. The section terminates in a series of thick-bedded, recrystallized fenestral limestones characterized by distinct and deeply penetrating paleokarstic features, pedogenic carbonates (calcretes), and some bauxites, which underlie a subaerial exposure surface representing a well known regional unconformity (Brlek et al., 2014). The unconformity, located at 46.5 m above the base of the section (Fig. 2B), is overlain by a middle Eocene succession of brackish-water limestones of the Kozina Member containing gastropods, which passes upward to open-ramp limestones with nummulitids making up the Foraminiferal Limestones unit, which is eventually overlain by a succession of the Dalmatian Flysch (Marjanac et al., 1998).

K–Pg planktonic foraminiferal biostratigraphy

The rare planktonic foraminifera contained in the complex massive deposit through the interval 15.50–20.32 m, and in the overlying muddy limestones are an unusual occurrence for an inner carbonate platform environment, which, however, are biostratigraphically useful (Fig. 2C). The presence of *Globotruncanella minuta* (Fig. 5A), *Gl. havanensis* (Fig. 5B), *Rugoglobigerina rugosa* (Fig. 5C), rare *Plummerita* cf. *Pl. hantkeninoides* (Fig. 5E), and *Muricohedbergella monmouthensis* indicates a terminal Maastrichtian age, i.e. the *Plummerita hantkeninoides* Zone (Li and Keller, 1998), which is here assigned to the Barren Interzone (cf. Arenillas et al., 2006, 2011), considering the occurrence of all these as reworked taxa within an event deposit. The overlaying red horizon from 20.30 to 20.32 m contains several Cretaceous forms such as *R. rugosa*, frequent *M. monmouthensis* (Fig. 5F), and very rare *Guembelitria* cf. *Gu. cretacea* (Fig. 5D). Very rare specimens of *Parvularugoglobigerina eugubina* syn. *longiapertura* (Fig. 5G), indicating a basal Paleocene Pα Zone, have been observed at 20.32 m. Co-occurrence of *M. monmouthensis*, *Pa. eugubina* syn. *longiapertura*, *Chiloguembelina midwayensis* (Fig. 5H), *Eoglobigerina eobulloides* (Fig. 5I), *Globanomalina planocompressa* (Fig. 5K), *Praemurica taurica* (Figs. 5L and 5M), and *Subbotina* cf. *S. trivialis* within the 50 cm interval above the red horizon indicates that this interval also belongs to the Pα Zone. However, considering the fact that it is difficult to distinguish between *Pa. longiapertura* and *Pa. eugubina* in thin section, the former defining the P0 Zone, and the first occurrence of the latter defining the Pα Zone (e.g., Premoli Silva et al., 2003), we assigned the interval 20.32–20.80 m to an indistinct P0-Pα Zones.

According to the biostratigraphic scheme of Premoli Silva et al. (2003), the last occurrence of *P. eugubina* 20.80 m marks the base of the P1 Zone, which is defined by the co-occurrence of *Ga. planocompressa*, *S.* cf. *S. trivialis* (Fig. 5N), and *E. eobulloides* up to 22.20 m. Planktonic foraminifera are present in six successive samples up to 28.35 m (Figs. 2B and 2C) but their rarity and poor preservation makes it impossible to make species-level identification, except for *S.* cf. *S. triloculinoides* (Fig. 5O) found in sample 28.35 m. Therefore, considering that *S. triloculinoides* spans the whole biostratigraphic zonal sequence from P1b to P3b (Premoli Silva et al., 2003), we place this interval provisionally in Zone P2, possibly extending to Zone P3.

Platinum group element composition and Re-Os isotope data

We have analyzed the platinum group element (PGE) contents in 9 horizons spanning the K–Pg interval (from meter level 15.30 to 25.26) at Majerovica, with particular attention to the interval across the red horizon at 20.30 m level, in search of possible K–Pg event geochemical signature. The results of our analysis are shown in Table 2, and Figs. 2D and 6.

A complete set of Re-Os data for samples from the Majerovica section (HMA) are listed in Table 3. Measured $^{187}Os/^{188}Os$ ratios were found to be extremely radiogenic, ranging from ~5.6 to ~6.8. Osmium concentrations range from 0.184 ppb (sample HMA13-18.00) to 0.571 ppb (sample HMA13-20.29A), roughly correlating with the Re contents, which are lowest in samples HMA13-18.00 and HMA13-20.10 (~3 ppb) and highest in sample HMA13-20.29 (~35 ppb). Re/Os ratios range from ~7 to ~62. Notably, there are some Os abundance differences between the analyses performed at Cardiff and Vienna (obtained by differing techniques, see Method section). Whereas Os concentrations from Vienna for most samples are consistently higher compared to the data obtained at Cardiff, we obtained comparable results for sample HMA13-20.10 (including the replicates A and B). Potentially, incomplete sample-spike equilibration of the vigorously reacting carbonate samples during initial acid treatment of the samples prior to solvent extraction may explain some of the differing results, but sample heterogeneity within the deposit samples may have contributed as well. The well-known nugget effect is particularly problematic for the PGE in sediments where only small sample masses are available (McDonald, 1998). However, in any case our results indicate extreme Re and Os compositional variations between the different limestone layers. Using the Re and Os concentrations, measured $^{187}Os/^{188}Os$ ratios and the known decay constant of ^{187}Re (see caption to Table 3 for details) we calculated the initial $^{187}Os/^{188}Os$ values at the time of the K–Pg boundary (66.0 Ma; Renne et al., 2013, and references therein).

DISCUSSION

Depositional mechanism of the massive deposit at Majerovica

The ~5 m thick breccia unit bears some general characteristics of a tsunami deposit (Morton et al., 2007) i.e., a tsunamite (e.g., Shiki et al., 2008). The presence of pelagic mudstone intraclasts containing terminal Cretaceous planktonic foraminifera suggests that the tsunami breached through and inundated the western margin of the carbonate platform, which was then located close to the present day island of Vis, some 40 km to the west of Hvar. In fact, the southwestern margin of the ACP was probably emergent during the Maastrichtian (Korbar, 2009). However, Maastrichtian slope to basinal facies recognized within the central Adriatic offshore of Croatia suggest a deep, east-striking embayment situated west of the island of Vis (Tari, 2002; Fig. 7B). The absence of any extraordinary sedimentary record within the supposed K–Pg boundary succession exposed on the northwestern coast of the island of Brač (Fig. 7B; Steuber et al., 2005), suggests that the tsunami did not come from a northeastern source.

It must have been a tsunami of such an amplitude that it was able to mobilize pelagic mudstone from the slope off the platform margin, mix it with platform-top mud-rich sediments, rip boulder-size blocks off the innermost platform, and redeposit all this chaotic sedimentary load (and probably associated organic material) over the flat inner platform after an eastward rush of tens of kilometers (Figs. 7A and 7B). The uneven upper surface of the breccia deposit suggests rapid deposition of the chaotic mixture of various carbonate platform sediments and sedimentary rocks in a highly viscous sediment flow (cf. cohesive flow of Mulder and Alexander, 2001). Assuming subtidal depths of 5-10 m (similar to the present-day Bahamas), such a flow in a shallow-water platform could be generated only by a large tsunami (Morton et al., 2007).

There has been debate on distinguishing between paleo-tsunami deposits and paleo-cyclone deposits using sedimentological criteria, but the ‘context’ (i.e., depositional setting) is of direct relevance for interpreting paleo-tsunami deposits (Shanmugam, 2012). Although most of the tsunami-related sedimentary signatures that have been observed within the Majerovica deposit (i.e., basal erosional surface, boulders, chaotic bedding, rip-up mud clasts) can be produced by other mechanism(s), it can also be argued that by considering the depositional setting for such an anomalous deposit, the evidence for a paleo-tsunami event becomes compelling.

It must be pointed out that the anomalous deposit at the K–Pg boundary at Majerovica is intercalated within typical innermost platform succession that yield neither a record of any tsunami nor of extraordinary storm event, as the section was probably situated tens of kilometers from the platform margin (Fig. 7B). An estimate of the extent of the Vis embayment would be at least 5 km from Majerovica, since there are no outcrops of the ACP deposits (i.e., the area between Vis and Hvar that is today covered by the Adriatic Sea). On the other hand, some coastal morphological features (e.g., deep embayments) may have helped to increase the amplitude of any tsunami (Gelfenbaum et al., 2011; Stefanakis et al., 2013). Thus, the embayment of Vis could have channelized and amplified a tsunami approaching from the west (Fig. 7B).

The lack of data on tsunami deposits from modern carbonate platform subtidal environments (Shiki et al., 2008) hampers comparison, but large quantities of suspended carbonate mud could have been an important factor in supporting such a far-travelling, erosive sediment flow. Apart from a possible role of the mud in this paleo-tsunami on Hvar, another crucial factor for such an anomalous deposit was probably the flow depth. Modern storm flow depths are commonly <3 m (3.7 m during the strongest modern cyclones; Hawkes and Horton, 2012), while the sedimentary load is deposited within a zone relatively close to the beach (up to a few hundreds of meters). By contrast, even millennium-scale modern tsunamis have flow depths greater than 10 m, and distribute the load over a broad region (Morton et al., 2007; Shiki et al., 2008). This observation also supports the interpretation that an unusually large tsunami (much larger than geologically frequent millennium-scale events) produced the anomalous deposit at Majerovica.

The truncations of laminae in the fine-grained sediment, making the upper part of the complex tsunami deposit (Fig. 2B), suggest synsedimentary consolidation of the underlying breccia deposit, seafloor turbulence, and wave action as the tsunami waves decrease in size. Envisioning a relatively flat platform top and probable lack of any significant backwash on this isolated carbonate platform, this fine-grained limestone was probably deposited under the influence of weak multidirectional currents produced by seiching after the tsunami surge within the subtidal environment. The unusually coarse clasts within this very fine-grained deposit may represent dropstones which could have fallen down to the seafloor from floating organic debris (cf. Doublet and Garcia, 2004), that must have been abundant after such a tsunami surge. The red-stained wackestone at the top, containing small intraclasts, and terminal Maastrichtian planktonic foraminifera is interpreted as an integral deposit of the tsunami event, possibly a late fall-out of the finest sediment particles from suspension, along with possible organic matter that could be diagenetically replaced by a sparite filling the undulating tiny laminae. The presence of species from a greater shelf depth (i.e., below the stormwave base) has often been observed in tsunami deposits and may represent a key diagnostic criterion to rule out storm wave deposition (Mamo et al. 2009). Moreover, the presence of pelagic microintraclasts containing planktonic foraminifera in the polygenic breccia at Majerovica is even better argument for a large tsunami that was able to mobilize off platform sediments deposited below the storm-weather wave-base, since rare planktonic specimens are found even in sand sheets deposited landward during modern tropical storm events (Hawkes and Horton, 2012).

The entire ACP has been thoroughly surveyed, especially during the production of the new Basic Geologic Map of Croatia (Vlahović et al., 2005; Korbar, 2009), but a similar deposit has not been recognized elsewhere. It is internally complex but still clearly intraformational, and thus differs from other breccias found within the ACP domain. For example, slump-related inner-platform breccias can form on when local tectonics coincides with a major drowning event, as reported from Cenomanian–Turonian successions in the nearby island of Brač (Korbar et al., 2012). Although there was impact-related cooling that lasted up to a few decades after the K–Pg boundary (Vellekoop et al., 2014), possible platform drowning would have been too short-lived to produce significant accommodation space for intra-platform redeposition of a 5 m thick polygenic breccia. Moreover, it does not contain any Paleocene planktonic foraminifera.

The earliest Danian "neoautochthon"

The contact at 20.32 m between this complex deposit and the overlying "neoautochthonous" mudstone is undulating but sharp and conformable (Figs. 3E and 4G). Some rare Cretaceous forms found in the lowermost part of the neoautochthon (Figs. 5C and 5D) may originate from locally redeposited tsunami sediment. Beside surviving Cretaceous species such as *Muricohedbergella monmouthensis* and rare

Guembelitria cf. *cretacea*, the mudstone at 20.32 m contains the first, rare basal Paleocene planktonic foraminifera *Parvularugoglobigerina eugubina* syn *longiapertura* (Figs. 2C and 5G), which define the indistinct P0-Pα zones up to 20.80 m (Fig. 2C). It must be pointed out, however, that the P0 Zone is rarely preserved even in pelagic successions due to the fact that it would be extremely thin in sedimentary settings with low accumulation rates in the order of mm/kyr, and subject to vertical mixing, reworking, and homogenization with overlying Pα sediment. At Gubbio for instance, where the K–Pg boundary was first defined on the basis of foraminiferal biostratigraphy by Luterbacher and Premoli Silva (1964), the P0 Zone is not recognizable, and the very first sediments of the basal Paleocene immediately overlying the Ir-rich K–Pg boundary clay layer are clumped into a unique P0-Pα Zones. P0-Pα condensation at Gubbio and in the nearby Ceselli section have also been reported (Arenillas, 1998; Arenillas and Arz, 2000).

According to recent time scales (e. g., Wade et al., 2011), the P0-Pα Zones spans some 200 kyr after the K–Pg boundary. However, high-resolution ^{3}He chemostratigraphic analysis across the K–Pg boundary interval at Gubbio (Mukhopadhyay et al., 2001) indicates a mean accumulation rate for the 55 cm thick P0-Pα Zones (i.e., the Eugubina Limestone; Coccioni et al., 2010) similar to that of the underlying terminal Maastrichtian pelagic limestone (about 10 mm/kyr); i.e, a duration for this zone of about 55 kyr. Moreover, preliminary results from a super-high-resolution (1 cm sampling), multiproxy cyclostratigraphic analysis of the Paleocene at Gubbio by Sinnesael et al. (2013) indicates a mean sedimentation rate for the first 1 m interval above the K–Pg boundary of 8.5 mm/kyr, thus a duration for the P0-Pα Zone of about 65 kyr. Similarly, on the basis of the high resolution planktonic foraminiferal biostratigraphy from the Mexican sections of Bochil and Guayal, Arenillas at al. (2006) estimated a duration for the P0-Pα Zones of about 60 to 70 kyr.

The muddy limestones overlaying this basal neoautochthon, contain inner-platform biota typical for the depauperate “Danian desert” (Gušić and Jelaska, 1990), along with some planktonic foraminifera, which define the successive early Paleocene biozones P1, and possibly P2. Such an unusual occurrence of planktonic foraminifera within a tropical inner-platform environment suggests that the shoals/reefs at the ACP margin were breached by a tsunami surge(s), allowing inflow from the open sea, prior to the recovery of a normal carbonate production and reef building biota during the earliest Paleocene (Vecsei and Moussavian, 1997).

Geochemical evidence /signature of the K–Pg event

In the Umbria-Marche basin of Italy, elevated concentrations of Ir within the 1-2 cm thick K–Pg boundary clay range from 1.2 ppb to 10.3 ppb among some 18 sections analyzed in the region (Montanari, 1991), compared to a background of about 0.02 ppb found in the pelagic limestones above and below the boundary (Alvarez et al., 1990). Through the lower 40 cm of the P0-Pα Zones at Gubbio, Ir concentrations drop to about 0.06 ppb, still a factor of 3 higher than background, but probably resulting from remobilization and vertical mixing caused by bioturbation (Montanari, 1991). According to the high-resolution ^{3}He chemostratigraphic analysis of Mukhopadhyay et al. (2001), the Ir-rich K–Pg boundary clay at Gubbio represents a duration of about 7 kyr.

At Majerovica (Hvar), the mean concentration of Ir from two replicated analyses is 0.55 ±0.06 ppb. This is not a strong anomaly compared with most K–Pg pelagic boundary sites around the world (e.g., Goderis et al., 2013) but considering the high-energy environment represented by this packstone, we suggest that this anomaly is sufficiently clear to be consistent with the impact signature. In fact, in all the known sections around the world where the K–Pg is associated with a tsunamite or a mass wasting deposit, Ir abundance does not exceed 1.0 ppb (Goderis et al., 2013). Here, however, that Pd, Pt, and Au abundances peak immediately above the red horizon at 20.32 m, some 20 cm above the Ir, Ru, Rh, and Os abundance peaks. This can be explained by different mobilities these elements may have experienced during diagenesis. Palladium, Pt, and Au are all more mobile than the other PGEs (e.g., Evans et al., 1993; Koeberl et al., 2012) and they just need to be mobilized a short distance and redeposited in a zone with contrasting pH/Eh conditions (i.e., the red-stained horizon) leading to the apparent discrepancy that present at Majerovica. Features like this have been observed in a number of different settings from other ejecta horizons to sediment-hosted mineral deposits and modern marine sediments (e.g., Colodner et al., 1992; Evans et al., 1993; De Vos et al., 2002; Simonson et al., 2009; Jowitt and Keays 2011 and references therein). Despite this possible influence of mobilization, PGE abundance ratios in the packstone layer (sample HMA 13-20.10) seem to be dominated by a meteoritic component. PGE ratios within this sample are consistently closer to the proposed chondritic component compared to all other samples in the interval between 18.00 and 20.32 m (Fig. 6). This, together with the Ir anomaly described above, provides strong evidence for an impact signature within the packstone.

The $^{187}Os/^{188}Os$ values (Table 3) are extremely radiogenic, with a spread between 5.4 and 6.7, resulting in unrealistic and contrasting values compared to any hypothetical Cretaceous and Paleogene sea water compositions (~0.4 to ~0.6; Peucker-Ehrenbrinck et al., 1995). Such $^{187}Os/^{188}Os$ ratios may point toward a significant modification of the sea water chemistry, possible due to local and enhanced influx of crustal material (typically exhibiting radiogenic $^{187}Os/^{188}Os$ ratios). For this reason, no definite statement about the presence of a meteoritic component can be made based on Os isotopic compositions, as the crustal input obscures any extraterrestrial contribution. The Re concentrations and $^{187}Re/^{188}Os$ ratios of the entire profile, although lowest in the packstone (sample HMA 13-20.10), both exceed values typical for the upper continental crust (~0.2 ppb Re and between ~20 to ~50 for $^{187}Re/^{188}Os$; Peucker-Ehrenbrinck and Jahn, 2001), demonstrating that the Re budget is unrelated to the impact event (chondrites usually exhibit $^{187}Re/^{188}Os$ ratios of ~0.4; e.g., Shirey and Walker, 1998). Instead, the observed concentrations require significant Re addition. The potential for authigenic enrichment of Re above crustal concentrations is greater than for many other elements (e.g., Crusius et al., 1996), especially under reducing conditions. Suboxic sediments, therefore, provide a sink for Re, making this element a useful tracer for redox conditions in continental margin sediments (e.g., Crusius et al., 1996).

Similar results were obtained in other studies as well. Brauns et al. (2001) measured extreme Re and Os compositional variations between different limestones of the upper Devonian "Kellwasser" horizon at the Frasnian/Famennian boundary (~367 Myr), which is assumed to record one of the most severe biological crises that occurred in the Phanerozoic. Re concentrations of up to 40 ppb and Os concentrations of up to 830 ppt, are comparable to our results, and very radiogenic $^{187}Os/^{188}Os$ ratios between ~1.2 and ~46 (corresponding to published $^{187}Os/^{186}Os$ ratios between 9.865 and 388.35) were also measured. These values were interpreted in favor of an absence of a meteoritic component at the Frasnian/Famennian boundary and the probable existence of a suboxic environment (Brauns et al., 2001). Moreover, Gordon et al. (2009) similarly concluded that highly radiogenic initial $^{187}Os/^{188}Os$ ratios calculated from measured Os isotope signatures of shales of the Frasnian/Famennian boundary at the La Serre section point toward secondary disturbance, masking any small meteoritic contributions.

In summary, the PGE interelement ratios support an impact signature within this relatively high-energy deposit (Figs. 2D and 6; Table 2), whereas Os isotopes and Re/Os ratios for samples from the Hvar K–Pg boundary (Table 3) neither support nor disprove the possible existence of an extraterrestrial component. Radiogenic $^{187}Os/^{188}Os$ and elevated Re/Os ratios within the packstone and across the whole profile are dominated by an enhanced clastic input into the sea water, as well as significant Re addition to the sediments in an anoxic milieu. Therefore, these results provide evidence for another interesting locality of enhanced input of crustal material to local and suboxic marine environments, which (besides the evidence found in limestones from the F-F boundary layer described above) are related to a global catastrophe.

Tsunami origin and possible link with the Chicxulub impact in Yucatan

Evidence of endogenic seismic activity and synsedimentary disturbances in Late Cretaceous–Paleocene time is found throughout the Umbria–Marche basin, and related eastern (Cònero) and southern (Abruzzo) carbonate platform margins (see Fig. 1C for location; Alvarez et al., 1985; Montanari, 1988; Montanari et al., 1989). In the Furlo and Genga depocenters of the Umbria-Marche basin, the Santonian to Danian succession of the pelagic Scaglia Rossa Formation is characterized by a sequence of calcareous seismo-turbidites made up of remobilized intrabasinal pelagic mud (Bice et al., 2007). In the Cònero and Montagna dei Fiori transitional facies of the basin, similar calcareous turbidites and massive calciruditic grain flows are made up of debris derived from carbonate aprons, which were festooning the margins of a small carbonate platform located at a short distance to the east of Monte Cònero, and the large Abruzzo carbonate platform to the south of the Montagna dei Fiori (Montanari et al., 1989). Yet, none of these localities preserves evidence of disturbances or seismic activity coincident with the K–Pg event. The Ir-rich K–Pg boundary clay layer is everywhere sandwiched between the undisturbed pelagic limestone of the *Abathomphalus majaroensis* Zone, and that of the overlying P0-Pα Zones (Montanari and Koeberl, 2000). Amalgamated turbidites at Furlo and Monte Cònero are found within the P1 Zone, some 60-80 cm above the K–Pg boundary. A similar situation is found in a Scaglia Rossa succession in western Sicily (Catalano et al., 1973). Therefore, whatever triggered those turbidites, a seismic event and/or a tsunami, must have happened tens of thousands of years after the impact event.

If the Majerovica tsunamite is a direct consequence of the Chicxulub impact in Yucatan, there are two possible scenarios for where the megawave(s) originated from: 1) the tsunami was generated by a western Tethys shelf/platform failure caused by earthquakes which were activated by an attenuated seismic wave triggered by the impact; or 2) the tsunami was generated on the eastern sides of the Cuban and/or Caribbean platforms (or the Florida promontory) and propagated eastward across the Atlantic Ocean, funneled into the western Tethys, and struck the western margin of the large Adriatic carbonate platform (Fig. 7A). In both scenarios, the tsunami would have reached the ACP within 24 hours after the impact, which a much shorter time than the settling of the finest-grained, non-ballistic impact fallout in such a distant region (Artemieva and Morgan, 2009). It follows that the PGE-enriched impact fallout would be found in the sediments above the K–Pg tsunamite, in the suspension fallout deposit and/or diluted in the neoautochthonous P0-Pα biomicrite due to vertical mixing. On the other hand, coarser-grained impact ejecta reaching the Adriatic region ballistically would have fallen out before the tsunami struck the ACP, and would be distributed sparsely within the massive tsunami deposit.

The first scenario requires that an attenuated seismic wave reached the western Tethys region with enough residual energy to trigger major earthquakes, causing mass-wasting of the margins of platforms or shorelines. Considering the possibility that the unusual deep-sea slumps at the K–Pg boundary from the offshore of Portugal (DSDP Site 398D; Norris et al., 2000; Norris and Firth, 2002) may have been caused by a seismically-induced collapse of the southwestern European continental margin, southeast-bound tsunamis may also have been triggered in the southeastern margins of the continental microplates of Corsica, Sardinia, Calabria, Kabilia, and Alboran, which were still attached to the southern margins of Europe (Rosenbaum et al., 2002, Advokaat et al., 2014; Figs. 1C and 7A). However, no evidence of any seismic or tsunami event is found in the complete and continuous outer-neritic GSSP section of El Kef, in Tunisia (Molina et al., 2006), nor in other marine sites in the region, most of which represent deeper-marine deposits (Smit, 1999). Most of the outer neritic successions of Tunisia, which faced the southern European margins, were probably protected from any direct (westerly) Atlantic tsunami by a region of exposed land, and lack sedimentary evidence for an incoming tsunami from the north (Adatte et al., 2002; Figs. 1C and 7A). On the other hand, the unusually coarse-grained deposit overlying the erosional surface at the tentatively placed K–Pg boundary within the inner neritic Seldja section (Fig. 1C, Adatte et al., 2002) suggests that evidence of tsunami deposition may still be present in shallow-water successions in the region.

Thus, the scenario of a tsunami that was generated in the margins of the western Atlantic, as a direct consequence of the Chicxulub impact event (Klaus et al., 2000; Norris et al., 2000; Norris and Firth, 2002; Claeys et al., 2002), which then propagated across the Atlantic Ocean (Fig. 7A), seems the more plausible. It may have entered the western Tethys through the then at least ~400 km wide Gibraltar strait, continuing its east-bound run across the unobstructed western Tethys ocean, passing by the north side of the Abruzzo carbonate platform, and finally striking the western margin of the Adriatic carbonate platform. Small carbonate banks located offshore of the Bahamas-type ACP, such as the small carbonate platform of Monte Cònero at the eastern margin of the Umbria–Marche basin (see Fig. 1C; Montanari et al., 1989; Montanari and Koeberl, 2000), and some others north of it, close to the western margin of the Adriatic platform (Korbar, 2009), were probably completely inundated. These small platforms were situated northwest of the deep embayment of Vis (Fig. 1C) which was on the predicted direct trajectory of the tsunami (Fig. 7B) and thus may have increased the run-up hight and the tsunami surge (cf. Gelfenbaum et al., 2011; Stefanakis et al., 2013) on that part of the ACP.

This finding on Hvar should stimulate further research of the Majerovica locality in more details, as well as possible re-investigation of the other successions in the region with special emphasis on potential tsunami evidence. If confirmed, this finding provides a new constraint for further modeling of the catastrophic aftermaths of the Chixculub impact at the Cretaceous–Paleogene boundary. The modeling could be important also for the debated western Tethyan paleogeographic and geodynamic reconstructions.

CONCLUSIONS

The Majerovica section at Hvar, Croatia, represents the first-recognized case of a sedimentary record across the K–Pg boundary, constrained by multiple, independent stratigraphical methods, in a tropical carbonate platform setting. We hypothesize that the unusual massive intraformational deposit and the overlying finer-grained sediment localized to this area represent a complex tsunamite deposited around the K–Pg boundary.

The elevated PGE abundances, including the Ir peak measured in the topmost part of the tsunamite, suggest a causal link with the Chicxulub impact event in Yucatan. The Os isotopic composition of the boundary samples is dominated, however, by an unusually high Re content, which, in turn, results in highly radiogenic Os isotope ratios that mask any possible extraterrestrial signature.

There is the lack of reported evidence for any major seismic and/or synsedimentary disturbance within slope and basinal successions during the K–Pg boundary interval in the peri-Adriatic region. Thus, the unusual sedimentary record at Hvar is interpreted to be the consequence of a major tsunami that was generated by the collapse(s) of the western Atlantic margins induced by the Chicxulub impact event.

ACKNOWLEDGMENTS

This work was supported by the Croatian Geological Survey at Zagreb, through MZOS project No. 181-1191152-2697. Dr. Dieter Buhl (Ruhr-Universität, Bochum, Germany) is thanked for the strontium isotopes analyses. We thank Mihovil Brlek for assistance in the field, and Orestina Francioni for preparing some extra 80 high quality thin sections in her specialized lab in Ancona (Italy). We thank the Association "Le Montagne di San Francesco" for supporting this research, Matthias Sinnesael (Free University of Brussels) for helping sampling in the field, Eliana Fornaciari (University of Padua), and Silvia Gardin (UPMC Paris) for assessing the total absence of calcareous nannofossils (a part from very rare and dubious *Thoracosphaera*), in samples HMA/13-20.30, 20.32, 20.50, and 20.80. We would like to thank GSAB editors David Schofield, Walter Alvarez, and Brian Pratt, as well as Jody Bourgeois, Ignacio Arenillas, Richard D. Norris, and an anonymous reviewer, for useful comments and suggestions on previous drafts of this paper.

REFERENCES CITED

Adatte, T., Keller, G., and Stinnesbeck, W., 2002, Late Cretaceous to early Paleocene climate and sea-level fluctuations: the Tunisian record: Palaeogeography, Palaeoclimatology, Palaeoecology, v. 178, p. 165-196.

Advokaat, E.L., van Hinsbergen, D.J.J., Maffione, M., Langereis, C.G, Vissers R.L.M., Cherchi, A., Schroeder, R., Madani, H., and Columbu, S., 2014, Eocene rotation of Sardinia, and the paleogeography of the western Mediterranean region: Earth and Planetary Science Letters, v. 401, p. 183-195.

Alvarez, L.W., Alvarez, W., Asaro, F., and Michel, H.V. 1980, Extraterrestrial cause for the Cretaceous-Tertiary extinction. Science, v. 208, p. 1095-1108.

Alvarez, W., Colacicchi, R., and Montanari, A., 1985. Synsedimentary slides and bedding formation in Apennine pelagic limestones: Journal of Sedimentary Petrolology, v. 55, p. 720-734.

Alvarez, W., Asaro, F., and Montanari, A., 1990, Ir profile for 10 Myr across the Cretaceous-Tertiary boundary at Gubbio (Italy): Science, v. 250, p. 1700-1702.

Alvarez,W., Claeys, P., and Kieffer, S.W., 1995, Emplacement of KT boundary shocked quartz from Chicxulub crater: Science, v. 269, p. 930-935.

Arenillas I., 1998, Biostratigrafía con foraminíferos planctónicos del Paleoceno y Eoceno inferior de Gubbio (Italia): calibración biomagnetoestratigráfica: Neues Jahrbuch für Geologie und Paläontologie, Monatshefte, 1998, no. 5, p. 299-320.

Arenillas, I., and Arz, J.A., 2000, *Parvularugoglobigerina eugubina* type-sample at Ceselli (Italy): planktic foraminiferal assemblage and lowermost Danian biostratigraphic implications: Rivista Italiana di Paleontologia e Stratigrafia, v. 106, p. 379-390.

Arenillas, I., Arz, J.A., Grajales-Nishimura, J.M., Murillo-Muñetón, G., Alvarez, W., Camargo-Zanoguera, A., Molina, E., and Rosales-Domínguez, C., 2006, Chicxulub impact event is Cretaceous/Paleogene boundary in age: new micropaleontological evidence: Earth and Planetary Science Letters, v. 249, p. 241-257.

Arenillas, I., Arz, J.A., Grajales-Nishimura, J.M., Rosales-Domínguez, M.C., Gónzalez-Lara, J.C., Maurrasse, F.J-M.R., Rojas-Consuegra, R., Murillo-Muñetón, G., Velasquillo-Martínez, L.G., Camargo-Zanoguera, A., and Menéndez-Peñate, L., 2011, Integrated stratigraphy of the Cretaceous-Tertiary transition in the Gulf of Mexico: key horizons for recognition of oil reservoirs: Gulf Coast Association of Geological Societies Transactions, v. 61, p. 33-44.

Artemieva N., and Morgan J., 2009, Modeling the formation of the K–Pg boundary layer, Icarus, v. 201, p. 768-780.

Berggren, W.A., and Pearson, P.N., 2005, A revised tropical to subtropical Paleogene planktonic foraminiferal zonation. Journal of Foraminiferal Research, v. 35, p. 279-298.

Bice, D.M., Montanari, A., and Rusciadelli, G., 2007, Earthquake-induced turbidites triggered by sea level oscillations in the Upper Cretaceous of Italy, Terra Nova, v. 18, p. 387-392.

Birck, J.L., Roy Barman, M., and Capmas, F., 1997, Re-Os isotopic measurements at the femtomole level in natural samples: Geostandards Newsletter**,** v. 21, p. 19-27.

Bosellini, A., Morsilli, M., and Neri, C., 1999, Long-term event stratigraphy of the Apulia platform margin (Upper Jurassic to Eocene, Gargano, southern Italy): Journal of Sedimentary Research, v. 69, p. 1241-1252.

Bralower, T.J., Paull, C.K., and Leckie, R.M., 1998, The Cretaceous-Tertiary boundary cocktail: Chicxulub impact triggers margin collapse and extensive sediment gravity flows: Geology, v. 26, p. 331-334.

Brauns, M., 2001, Osmium isotopes and the Upper Devonian "Kellwasser" event: American Geophysical. Union, Fall Meeting 2001, abstract IP11A-0663.

Brlek, M., Korbar, T., Košir, A., Glumac, B., Grizelj, A., and Otoničar, B., 2014, Discontinuity surfaces in Upper Cretaceous to Paleogene carbonates of central Dalmatia (Croatia): *Glossifungites* ichnofacies, biogenic calcretes and stratigraphic implications: Facies, v. 60, p. 467-487.

Catalano, R., Maniaci, G., Renda, P., and Urso, G., 1973, Un esempio di evoluzione sedimentaria nelle facies di bacino dei monti di Palermo: la successione mesozoica-terziaria di Cala Rossa (Terrasini): Geologica Romana, v. 12, p. 151-175.

Channell, J.E.T., D'Argenio, B., and Horvath, F., 1979, Adria, the African promontory in Mesozoic Mediterranean palaeogeography: Earth-Science Reviews, v. 15, p. 231-292.

Claeys P. H., Kiessling W. and Alvarez W., 2002, Distribution of Chicxulub ejecta at the Cretaceous-Tertiary boundary, *in* Koeberl, C., and MacLeod, K.G., eds., Catastrophic Events and Mass Extinctions: Impacts and Beyond: Geological Society of America Special Paper 356, p. 55-68.

Coccioni, R., Frontalini, F., Bancalà, G., Fornaciari, E., Jovane, L., and Sprovieri, M., 2010, The Dan-C2 hyperthermal event at Gubbio (Italy): Global implications, environmental effects, and cause(s): Earth and Planetary Science Letters, v. 297, p. 298-305.

Cohen A.S. and Waters, F.G., 1996, Separation of osmium from geological materials by solvent extraction for analysis by thermal ionization mass spectrometry: Analytica Chimica Acta, v. 332, p. 269-275.

Colodner, D.C., Boyle, E.A., Edmond, J.M., and Thomson, J., 1992, Post-depositional mobility of platinum, iridium and rhenium in marine sediments: Nature, v. 358, p. 402-404.

Ćosović, V., Drobne, K. and Moro, A., 2004. Paleoenvironmental model for Eocene foraminiferal limestones of the Adriatic carbonate platform (Istrian Peninsula): Facies, v. 50, p. 61–75.

D'Argenio, B., 1970, Evoluzione geottettonica comparata tra alcune piattaforme carbonatiche dei Mediterranei Europeo ed Americano: Atti Accademia Pontiana, v. 20, p. 3-34.

Dercourt, J., Ricou, L.E., and Vrielynck, B., eds., 1993, Atlas Tethys Palaeoenvironmental Maps: Paris, Gauthier Villars, 307 p.

De Vos, E., Edwards, S.J., McDonald, I., Wray, D.S., and Carey, P., 2002, Distribution and origin of platinum-group elements in contemporary fluvial sediments in the Kentish Stour, UK. Applied Geochemistry: v. 17, p. 1115-1121.

Doublet, S., and Garcia, J-P., 2004, The significance of dropstones in a tropical lacustrine setting, eastern Cameros Basin (Late Jurassic-Early Cretaceous, Spain): Sedimentary Geology, v. 163, p. 293-309.

Drobne, K., Ogorelec, B., Pleničar, M., Barattolo, F., Turnšek, D., and Zucchi-Stolfa, M.L., 1989, The Dolenja Vas section, a transition from Cretaceous to Paleocene in the NW Dinarides, Yugoslavia: Memorie della Società Geologica Italiana, v. 40, p. 73-84.

Eberli, G.P., Bernoulli, D., Sanders, D., and Vecsei, A., 1993, From aggradation to progradation: the Maiella platform (Abruzzi, Italy), *in* Simo, A.J. Scott, R.W., and Masse, J.-P., eds., Cretaceous carbonate platforms: Memoirs of the American Association of Petroleum Geologists, v. 56, p. 213-232.

Evans, N.J., Grégoire, D.C., Grieve, R.A.F., Goodfellow, W.D., and Veizer, J., 1993, Use of platinum-group elements for impactor identification: terrestrial impact craters and the Cretaceous-Tertiary boundary: Geochimica et Cosmochimica Acta, v. 57, p. 3737-3748.

Fornaciari, E., Giusberti, L., Luciani, V., Tateo, F., Agnini, C., Backman, J., Oddone, M., and Rio, D., 2007, An expanded Cretaceous-Tertiary transition in a pelagic setting of the Southern Alps (central-western Tethys): Palaeogeogrraphy Palaeoclimatology, Palaeoecoleoecology, v. 255, p. 98-131.

Gelfenbaum, G., Apotsos, A, Stevens, A.W., and Jaffe, B., 2011, Effects of fringing reefs on tsunami inundation: American Samoa: Earth-Science Reviews, v. 107, p. 12-22.

Goderis, S., Paquay, F., and Claeys, P. 2013, Projectile identification in terrestrial impact structures and ejecta material, *in* Osinski, G. and Pierazzo E., eds., Impact Cratering: Processes and Products: Wiley-Blackwell, p. 223-239.

Gordon, G.W., Rockman, M., Turekian, K.K., and Over, J., 2009, Osmium isotopic evidence against an impact at the Frasnian/Famennian boundary: American Journal of Science, v. 309, p. 420-430.

Govindaraju, K., 1994. 1994 compilation of working values and samples description for 383 geostandards: Geostandards Newsletter, v. 18, p. 1-158.

Gušić, I., and Jelaska, V., 1990, Stratigrafija gornjokrednih naslaga otoka Brača u okviru geodinamske evolucije Jadranske karbonatne platforme (Upper Cretaceous stratigraphy of the Island of Brač within the geodynamic evolution of the Adriatic carbonate platform): Djela Jugoslavenske akademije znanosti i umjetnosti. v. 69, 160 p.

Hawkes, A.D., and Horton, B.P., 2012, Sedimentary record of storm deposits from Hurricane Ike, Galveston and San Luis Islands, Texas: Geomorphology, v. 171-172, p. 180-189.

Howarth, R.J., and McArthur, J.M., 1997, Statistics for strontium isotope stratigraphy: a robust LOWESS fit to the marine strontium isotope curve for the period 0 to 206 Ma, with look-up table for the derivation of numerical age: Journal of Geology, v. 105, p. 441-456.

Huber, B.T., and Leckie, R.M., 2011, Planktic foraminiferal species turnover across deep-sea Aptian/Albian boundary sections: Journal of Foraminiferal Research, v. 41, 53-95.

Huber, H., Koeberl, C., McDonald, I., and Reimold, W.U., 2001, Geochemistry and petrology of Witwatersrand and Dwyka diamictites from South Africa: search for an extraterrestrial component: Geochimica et Cosmochimica Acta, v. 65, p. 2007-2016.

Huber, B.T., MacLeod, K.G., Norris, R.D., 2002, Abrupt extinction and subsequent reworking of Cretaceous planktonic foraminifera across the Cretaceous-Tertiary boundary: Evidence from the subtropical North Atlantic, *in* Koeberl, C., and MacLeod K.G., eds., Catastrophic Events and Mass Extinctions: Impacts and Beyond: Geological Society of America Special Paper 356, p. 277-289.

Jowitt, S.M., and Keays, R.R., 2011, Shale-hosted Ni-(Cu-PGE) mineralization: a global review: Applied Earth Science (Transactions Institute of Mining & Metallurgy Section B), v. 120, p. 187-197.

Kiyokawa, S., Tada, R., Iturralde-Vinent, M.A., Tajika, E., Yamamoto, S., Oji, T., Nakano, Y., Goto, K., Takayama, H., Garcia-Delgado, D., Diaz-Otero, C., Rojas-Consuegra, R., and Matsui, T., 2002, Cretaceous-Tertiary boundary sequence in the Cacarajicara Formation, western Cuba: An impact-related, high-energy, gravity flow deposit, *in* Koeberl, C., and MacLeod, K.G., eds., Catastrophic Events and Mass Extinctions: Impacts and Beyond: Geological Society of America, Special Paper 356, p. 125-144.

Klaus, A., Norris, R.D., Kroon, D., and Smit, J., 2000, Impact-induced K-T boundary mass wasting across the Blake Nose, W. North Atlantic: Geology, v. 28, p. 319-322.

Koeberl, C., Claeys, P., Hecht, L., and McDonald, I., 2012, Geochemistry of impactites: Elements, v. 8, p. 37-42.

Korbar, T., 2009, Orogenic evolution of the External Dinarides in the NE Adriatic region: a model constrained by tectonostratigraphy of Upper Cretaceous to Paleogene carbonates: Earth-Science Reviews, v. 96, p. 296-312.

Korbar, T., Cvetko Tešović, B., Radovanović, I., Krizmanić, K., Steuber, T., and Skelton, P.W., 2010, Campanian *Pseudosabinia* from the Pučišća Formation on the Island of Hvar (Adriatic Sea Croatia): Turkish Journal of Earth Sciences, v. 19, p. 721–731.

Korbar, T., Glumac, B., Cvetko Tešovic, B., and Cadieux, S.B., 2012, Response of a carbonate platform to the Cenomanian-Turonian drowing and OAE2: a case study from the Adriatic Platform (Dalmatia, Croatia): Journal of Sedimentary Research, v. 82, p. 163-176.

Li, L., and Keller, G., 1998, Diversification and extinction in Campanian-Maastrichtian planktic foraminifera of northwestern Tunisia: Eclogae geologicae Helvetiae, v. 91, p. 75-102.

Lirer, F., 2000, A new technique for retrieving calcareous microfossils from lithified lime Deposits: Micropaleontology, v. 46, p. 365-369.

Lodders, K., 2003, Solar system abundances and condensation temperatures of the elements: Astrophysical Journal, v. 591, p.1220-1247.

Luterbacher, H.P., and Premoli Silva, I., 1964, Stratigrafia del limite Cretacico-Terziario nell'Appennino centrale: Rivista Italiana di Paleontologia e Stratratigrafia, v. 70, p. 68-128.

Mamo, B., Strotz, L., and Dominey-Howes, D., 2009, Tsunami sediments and their foraminiferal assemblages: Earth-Science Reviews, v. 96, 263-278.

Marjanac, T., Babac, D., Benić, J, Ćosović, V., Drobne, K., Marjanac, Lj., Pavlovec, R., and Velimirović, Z., 1998, Eocene carbonate sediments and sea-level changes on the SE part of Adriatic Carbonate Platform (Island of Hvar and Pelješac Peninsula, Croatia), *in* Hottinger L., and Drobne K., eds., Paleogene shallow benthos of the Tethys: Dela, Slovenska akademija znanosti in umetnosti (SAZU), v. 34, p. 243-254.

McArthur, J.M., Howarth, R.J., and Bailey, T.R. 2001, Strontium isotope stratigraphy: lowess version 3. Best-fit to the marine Sr-isotope curve for 0 to 509 Ma and accompanying look-up table for deriving numerical age: Journal of Geology, v. 109, p. 155-170.

McDonald, I., 1998, The need for a common framework for collection and interpretation of data in platinum-group element geochemistry: Geostandards Newsletter, v. 22, p. 85-91.

McDonald, I., and Viljoen, K.S., 2006, Platinum-group element geochemistry of mantle eclogites: a reconnaissance study of xenoliths from the Orapa kimberlite, Botswana: Applied Earth Science (Transactions Institute of Mining & Metallurgy Section B), v. 115, p. 81-93.

Meisel, T., and Moser, J., 2004, Reference materials for geochemical PGE analysis: new analytical data for Ru, Rh, Pd, Os, Ir, Pt and Re by isotope dilution ICP-MS in 11 geological reference materials: Chemical Geology, v. 208, p. 319-338.

Molina, E., Alegret, L., Arenillas, I.,.et al., 2006, The Global Boundary Stratotype Section and Point for the base of the Danian Stage (Paleocene, Paleogene, "Tertiary", Cenozoic) at El Kef, Tunisia: original definition and revision: Episodes, v. 29, p. 263-273.

Montanari, A., 1988, Tectonic implications of hydrothermal mineralizations in the Late Cretaceous-Early Tertiary pelagic basin of the Northern Apennines: Bollettino della Società Geologica Italiana, v. 107, p. 399-411.

Montanari, A., 1991, Authigenesis of impact spheroids in the K/T boundary clay from Italy: new constraints for high-resolution stratigraphy of terminal Cretaceous events: Journal of Sedimentary Petrology, v. 61, p. 315-339.

Montanari, A., and Koeberl, C., 2000. Impact Stratigraphy: The Italian Record: Lecture Notes in Earth Sciences, no. 93, Springer, Heidelberg, p. 1-364.

Montanari, A., Chan, L.S., and Alvarez, W., 1989, Synsedimentary tectonics in the Late Cretaceous-Early Tertiary pelagic basin of the Northern Apennines, *in* Crevello, P., Wilson, J.L., Sarg, R. and Reed, F., eds., Controls on Carbonate Platforms and Basin Development: SEPM Special Publication, v. 44, p. 379-399.

Morton, R.A., Gelfenbaum, G., and Jaffe, B.E., 2007, Physical criteria for distinguishing sandy tsunami and storm deposits using modern examples: Sedimentary Geology, v. 200, p. 184-207.

Mukhopadhyay, S., Farley, K.A., and Montanari, A., 2001, A short duration of the Cretaceous-Tertiary boundary event: Evidence from extraterrestrial Helium-3: Science, v. 291, p. 1952-1955.

Mulder, T., and Alexander, J., 2001, The physical character of subaqueous sedimentary density flows and their deposits: Sedimentology, v. 48, p. 269-299.

Norris, R.D., 2001, Impact of K-T boundary events on marine life, *in* Briggs, D.E.G. and Crowther, P.R., eds., Paleobiology II: Blackwell Press, p. 229–231.

Norris, R.D., and Firth, J., 2002, Mass wasting of Atlantic continental margins following the Cicxulub impact event, *in* Koeberl, C., and MacLeod, K.G., eds., Catastrophic Events and Mass Extinctions: Impacts and Beyond: Geological Society of America Special Paper 356, p. 79-95.

Norris, R.D., Firth, J., Blusztajn, J., and Ravizza, G., 2000, Mass failure of the North Atlantic margin triggered by the Cretaceous/Paleogene bolide impact: Geology, v. 28, p. 1119-1122.

Ogorelec, B., Dolenec, T., and Drobne, K., 2007. Cretaceous-Tertiary boundary problem on shallow carbonate platform: Carbon and oxygen excursions, biota and microfacies at the K/T boundary section Dolenja Vas and Sopada in SW Slovenia, Adria CP: Palaeogeography, Palaeoclimatology, Palaeoecology, v. 255, p. 64-76.

Olsson, R.K., Hemleben, C., Berggren, W.A., and Huber, B.T., 1999, Atlas of Paleocene planktonic foraminifera: Smithsonian Contributions to Paleobiology: Washington, D.C., Smithsonian Institution Press, 252 p.

Peucker-Ehrenbrink, B. and Ravizza, G., 1995, The marine Osmium isotope record: Terra Nova, v. 12, p. 205-219.

Peucker-Ehrenbrinck, B., and Jahn B.M., 2001, Rhenium-osmium isotope systematics and platinum group element concentrations: Loess and the upper continental crust. Geochemistry, Geophysics, Geosystems, v. 2, 1061, doi: 10.1029/2001GC000172.

Premoli Silva, I., Rettori, R., and Verga, D., 2003, Practical manual of Paleocene and Eocene planktonic Foraminifera: Department of Earth Sciences, University of Perugia, Italy, 1-152 p.

Renne, P.R., Deino, A.L., Hilgen, F.J., Kuiper, K.F., Mark, D.F., Mitchell III, W.S., Morgan, L.E., Mundil, R. and Smit, J., 2013, Time scales of critical events around the Cretaceous-Paleogene Boundary: Science, v. 339, p. 684-687.

Rosenbaum, G., Lister, G.S., and Dubois, C., 2002, Reconstruction of the tectonic evolution of the western Mediterranean since the Oligocene, *in* Rosenbaum, G.

and Lister, G.S., eds., Reconstruction of the evolution of the Alpine-Himalayan Orogen: Journal of the Virtual Explorer, v. 8, p. 107-130.

Schlüter, M., Steuber, T., Parente, M., and Mutterlose, J., 2008, Evolution of a Maastrichtian-Paleocene tropical shallow-water carbonate platform (Qalhat, NE Oman): Facies, v. 54, p. 513-527.

Schulte, P., and 44 al., 2010, The Chicxulub asteroid impact and mass extinction at the Cretaceous-Paleogene Boundary: Science, v. 327, p. 1214-1218.

Shanmugam, S., 2012, Process-sedimentological challenges in distinguishing paleo-tsunami deposits: Natural Hazards, v. 63, p. 5-30.

Shiki, T., Tsuji, Y., Yamazaki, T., and Minoura, K., 2008, Tsunamiites - Features and Implications: Developments in Sedimentology Series, Elsevier, Amsterdam, 411 p.

Shirey, S.B. and Walker, R.J., 1998, The Re-Os isotope system in cosmochemistry and high-temperature geochemistry: Annual Review of Earth and Planetary Sciences, v. 26, p. 423-500.

Simonson, B.M., McDonald, I., Shukolyukov, A., Koeberl, C., Reimold, W.U., and Lugmair, G., 2009, Geochemistry of 2.63-2.49 Ga impact spherule layers and implications for stratigraphic correlations and impact processes: Precambrian Research, v. 175, p. 51-76.

Sinnesael M., De Vleeschouwer D., Montanari A., Coccioni R., and Claeys P., 2013, The astronomical influence on climate change across the KT boundary: A cyclostratigraphic study of the late Maastrichtian - early Paleocene in the Umbria-Marche Basin (Apennine mountains, central Italy): Poster in the workshop "Transient Changes in Past Climates on the 10th Cioppino Conference", Urbino Summer School in Paleoclimatology, July 21, 2013, Urbino, Italy.

Smit, J., 1982, Extinction and evolution of planktonic Foraminifera after a major impact at the Cretaceous/Tertiary boundary, *in* Silver, L.T., and Schultz, P.H., eds., Geological Implications of Impacts of Large Asteroids and Comets on the Earth: Geological Society of America, Special Paper 190, p. 329-352.

Smit, J., 1999, The global stratigraphy of the Cretaceous-Tertiary boundary impact ejecta: Annual Review of Earth and Planetary Sciences, v. 27, p. 75-113.

Smit, J., and Hertogen, J., 1980, An extraterrestrial event at the Cretaceous-Tertiary boundary: Nature, v. 28, p. 198-200.

Smoliar, M. I., Walker, R. J., and Morgan, J.W., 1996, Re-Os ages of group IIA, IIIA, IVA, and IVB iron meteorites: Science, v. 271, p. 1099-1102.

Stefanakis, T.S., Contal, E., Vayatis, N., Dias, F. and Synolakis, C.E., 2013, Can small islands protect nearby coasts from tsunamis? An active experimental design approach: Cornell University Library, Physics Fluid Dynamics arXiv:1305.7385v1 [physics.flu-dyn], p. 1-20.

Steuber, T., Mitchell, S.F., Buhl, D., Gunter, G., and Kasper, H.U., 2002, Catastrophic extinction of Caribbean rudist bivalves at the Cretaceous-Tertiary Boundary: Geology, v. 30, p. 999–1002.

Steuber, T., Korbar, T., Jelaska, V., and Gušić, I., 2005, Strontium-isotope stratigraphy of Upper Cretaceous platform carbonates of the Island of Brač (Adriatic Sea, Croatia): implications for global correlation of platform evolution and biostratigraphy: Cretaceous Research, v. 26, p. 741–756.

Tari, V., 2002, Evolution of the northern and western Dinarides: a tectonostratigraphic approach; European Geosciences Union, Stephan Mueller Special Publication Series, 1, p. 223-236.

Tredoux, M., and McDonald, I., 1996, Komatiite WITS-1, low concentration noble metal standard for the analysis of non-mineralized samples: Geostandard Newsletter, v. 20, p. 267-276.

Vecsei, A., and Moussavian, E., 1997, Paleocene reefs on the Maiella platform margin, Italy: An example of the effects of the Cretaceous/Tertiary boundary events on reefs and carbonate platforms: Facies, v. 36, p. 123-140.

Vellekoop, J., Sluijs, A., Smit, J., Schouten, S., Weijers, J.W.H., Sinninghe Damsté, J.S., and Brinkhuis, H., 2014, Rapid short-term cooling following the Chicxulub impact at the Cretaceous–Paleogene boundary: Proceedings of the National Academy of Sciences, v. 111, p. 7537–7541.

Vlahović, I., Tišljar, J., Velić, I., and Matičec, D., 2005, Evolution of the Adriatic Carbonate Platform: palaeogeography, main events and depositional dynamics: Palaeogeography, Palaeoclimatololgy, Palaeoecology, v. 220, p. 333–360.

Wade, B.S., Pearson, P.N., Berggren,W.A., and Pälike, H., 2011, Review and revision of Cenozoic tropical planktonic foraminiferal biostratigraphy and calibration to the geomagnetic polarity and astronomical time scale: Earth-Science Reviews, v. 104, p. 111-142.

Zappaterra, E., 1994, Source rock distribution model of the Periadriatic region: Bulletin of the American Association of Petroleum Geologists, v. 78, p. 333-354.

FIGURE CAPTIONS

Figure 1 - A) Geographic map and main orogenic fronts of the western Mediterranean region, and B) location of the Majerovica section (HMA) in the southwestern side of the island of Hvar in the Dalmatian archipelago. C) Maastrichtian paleogeography of the western Mediterranean region, simplified and redrawn from Dercourt et al. (1993), Rosenbaum et al. (2002), and Adatte et al. (2002).

Figure 2 - Integrated stratigraphy of the K–Pg section at Majerovica: A) Panoramic view of the key outcrop; B) Chronostratigraphy, lithostratigraphy, and sedimentary facies; C) Diagnostic planktonic foraminifera taxa occurrences as identified in thin section, and relative biostratigraphic assessment; D) Stratigraphic distribution of PGE and gold abundances.

Figure 3 – Macrofacies of the K–Pg section of Majerovica. A) Erosional contact between the inner platform reddish microbial laminite/wackestone and the overlying polygenic breccia at meter level 15.50; B) Texture of the polygenic, matrix-supported carbonate breccia exposed at meter level 17.5; C) Texture of the polygenic, matrix-supported carbonate breccia that includes a >50 cm long ripped-up boulder of the underlying ostracode wackestone, well exposed at eastern coast of the Majerovica cove; D) Intraclast, possibly a dropstone, in the fine grained sediment immediately overlying the breccia unit at about meter level 20; E) The fine grained packstone underlying a ~2 cm thick red-stained laminated wackestone at meter level 20.30, which separates it from the overlying mudstone containing rare basal Danian planktonic foraminifera; F) Polished slab of the uppermost part of the packstone and the overlaying red-stained laminated wackestone (the contact at meter level 20.30 - topmost part of the tsunami deposit).

Figure 4 - Microfacies of the Majerovica K–Pg peritidal limestones (thin section

micro-photographs): A) Peloidal packstone with *Rhapydionina liburnica* and miliolid tests (0.90 m); B) Ostracod wackestone underlaying the lower erosional boundary of the K–Pg deposit (15.35 m); C) Lowermost part of the tsunamite characterized by a chaotic mixture of lithified lime mud, peloidal silt and mm to cm sized bioclasts in intraclastic-bioclastic-peloidal packstone-grainstone containing various limestone lithotypes, bioclasts, miliolids etc. (15.50 m); D) Small intraclast (dark area in the central-lower part of the microphotograph) of a biomicrite containing Maastrichian planktonic foraminifera (magnification in Fig. 5A) within the tsunami deposit (15.50 m); E) Bioclastic wackestone containing fragments of various thin-shelled bivalves, miliolids, ostracods, calcispheres, and planktonic foraminifera (17.50 m); F) mm thick laminae of peloidal-bioclastic packstone-grainstone (left) and peloidal-microbioclastic wackestone-packstone (right), characterized by lateral truncations (20.00 m); G) The meter level 20.32 at the contact of the underlaying red-stained laminated wackestone (top tsunamite) and the overlaying mudstone "neoautochthon". In the lower part, microbioclastic and intraclastic wackestone containing Maastrichtian planktonic foraminifera in the matrix (see Fig. 5), alternates with irregular and undulating laminoid sparite; H) Microbioclastic mudstone-wackestone and a burrow infill with peloidal-skeletal wackestone-packstone containing tiny miliolids, discorbids, other benthic foraminifera, ostracods, and rare planktonic foraminifera (20.50 m).
All bars = 1000 µm;

Figure 5 - Thin section micro-photographs of diagnostic planktonic foraminifera of the Majerovica K–Pg limestones (stratigraphic distribution in Fig. 2C): A) *Globotruncanella minuta* (15.50 m); B) *Globotruncanella havanensis* (20.30 m); C) *Rugoglobigerina rugosa* (20.32 m); D) *Guembelitria* cf. *cretacea* (20.32 m); E) *Plummerita* cf. *hantkeninoides* (20.30 m); F) *Muricohedbergella monmouthensis* (20.32 m); G) *Parvularugoglobigerina eugubina* syn. *longiapertura* (20.32 m); H) *Chiloguembelina midwayensis* 20.80 m); I) *Eoglobigerina eobulloides* (20.50 m); J) *Parasubbotina* cf. *pseudobulloides* (20.50 m); K) *Globanomalina planocompressa* (20,80 m); L, M) *Praemurica taurica* 20.50 m); N) *Subbotina* cf. *trivialis* (21.50 m); O) *Subbotina* cf. *triloculinoides* (28.35 m).
Figures: A, N bar = 50 µm, all others bar = 100 µm.

Figure 6 - CI chondrite normalized platinum group from the Majerovica samples, exemplifying the meteoritic contamination of the packstone (sample HMA 13-20.10) CI chondrite normalization values are from Lodders (2003).

Figure 7 Simplified Maastrichtian paleogeography of: A) the Caribbeans, Atlantic, and Western Tethys regions, simplified and redrawn from Dercourt et al. (1993), Rosenbaum et al. (2002), and Adatte et al. (2002), showing the location of sites with evidences for tsunamites, turbidites, seismites, or mass waste deposits related to the Chicxulub impact event (after Claeys et al., 2002), the location of the K–Pg tsunamite site at Hvar (star), and the hypothetical traces of the east-propagating tsunami triggered by the impact; B) the central Adriatic offshore of Croatia (cf. Tari, 2002; Korbar, 2009, and references therein), showing also the contours of the present day central Dalmatian islands (dotted lines).

Figure 1
Click here to download Figure: GSAB_B31084R4_Fig.1-locmap.pdf

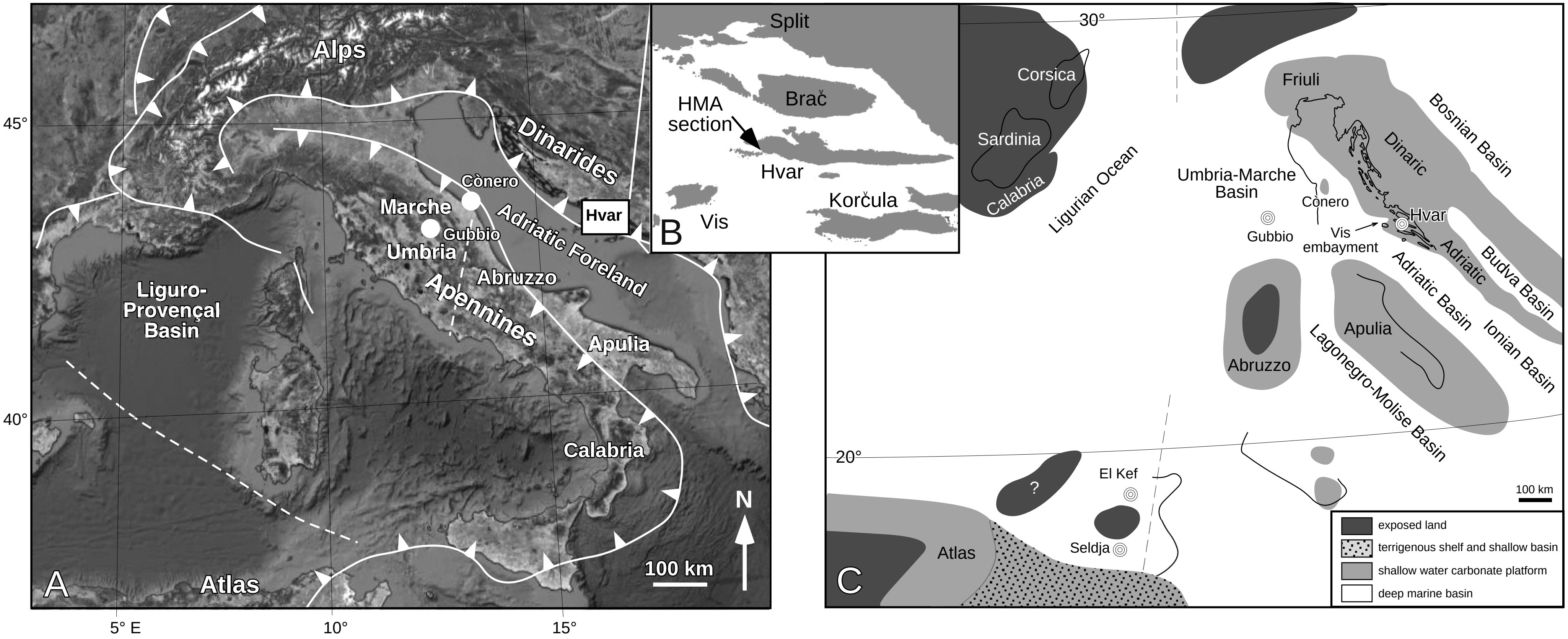

Figure 2

Click here to download Figure: GSAB_B31084R2_Fig2-stratigraphy.pdf

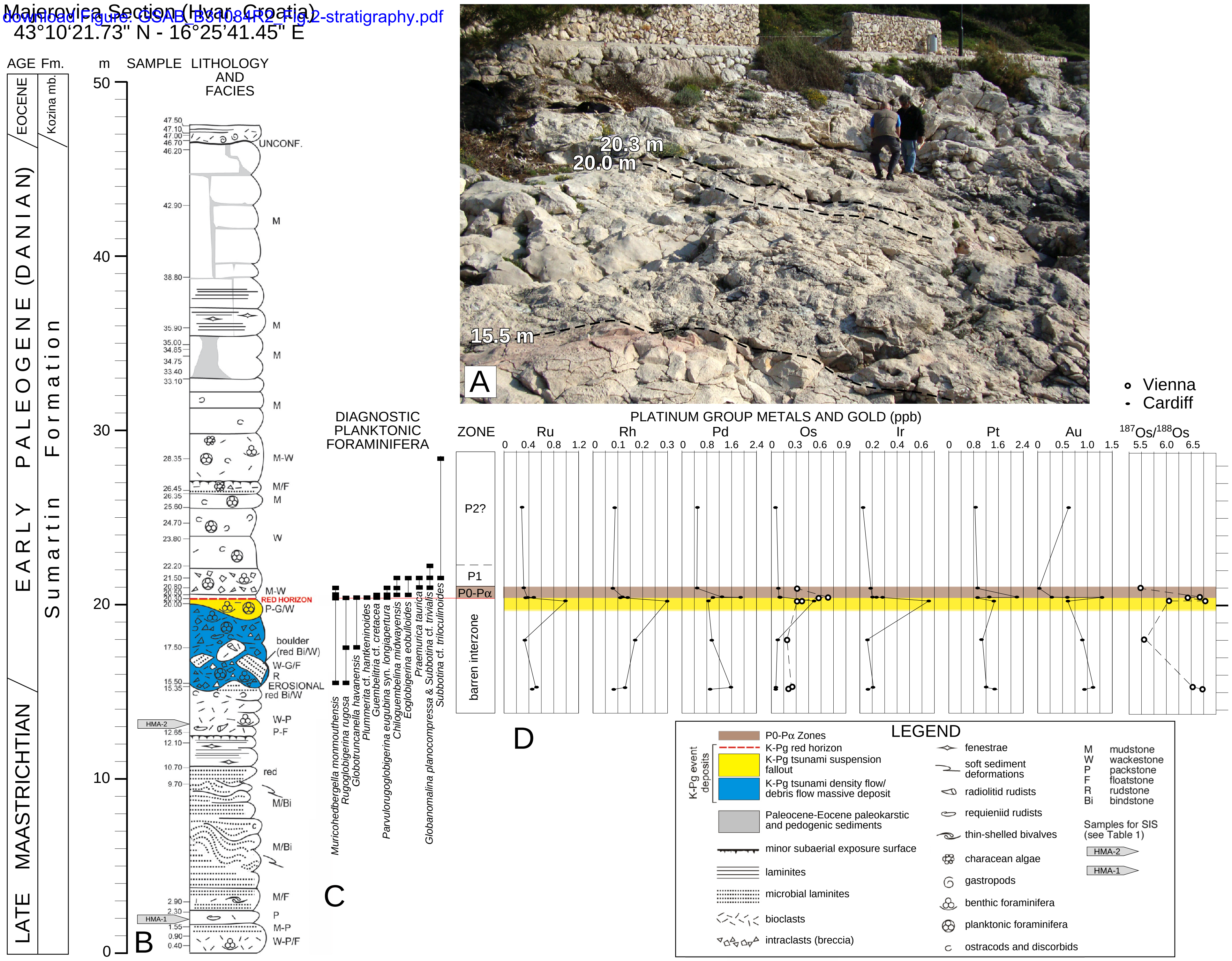

Figure 3

Click here to download Figure: GSAB_B31084R4_Fig.3-macrofacies.pdf

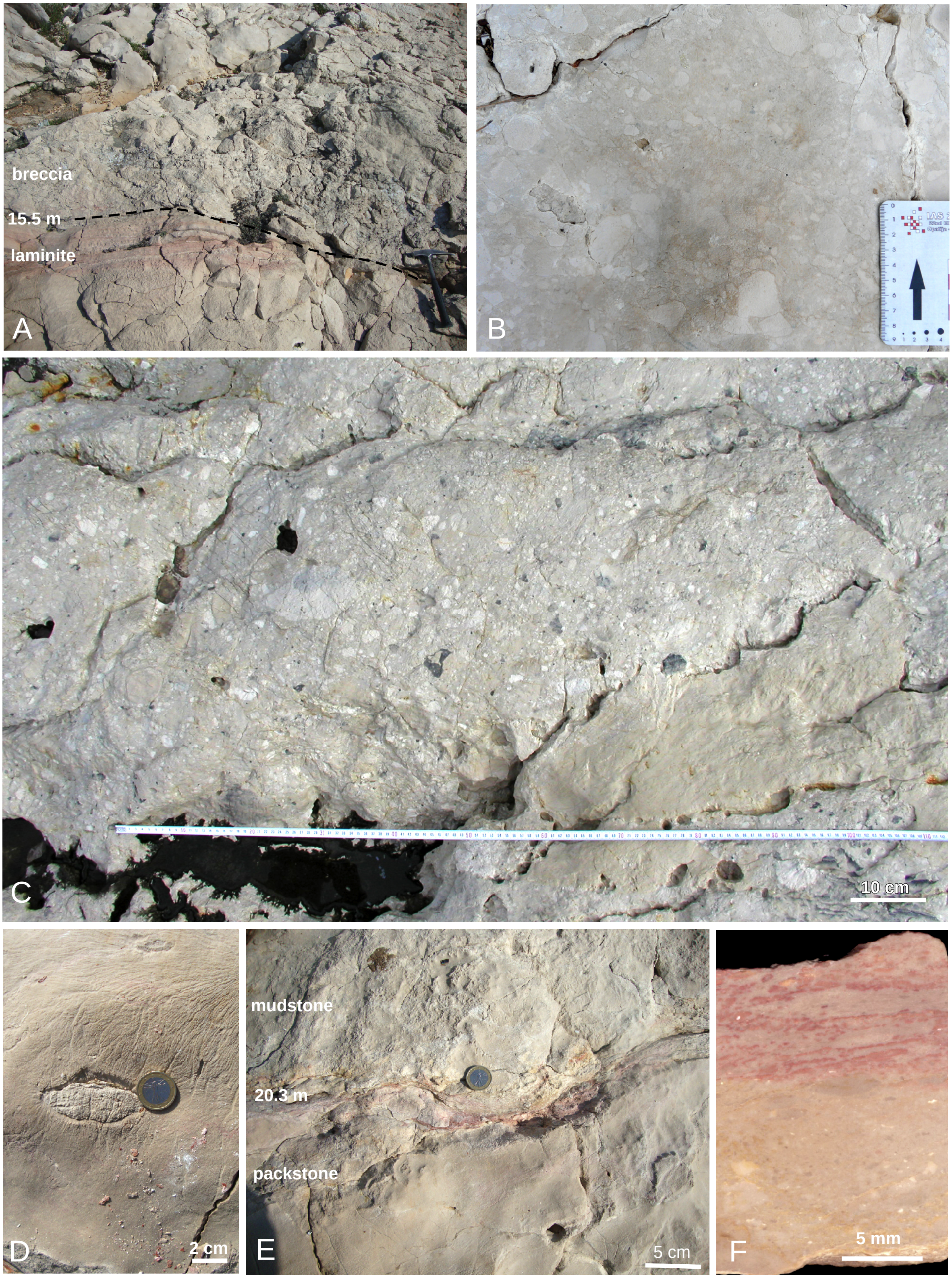

Figure 4

Click here to download Figure: GSAB_B31084_REV1_Fig.3_microfacies.pdf

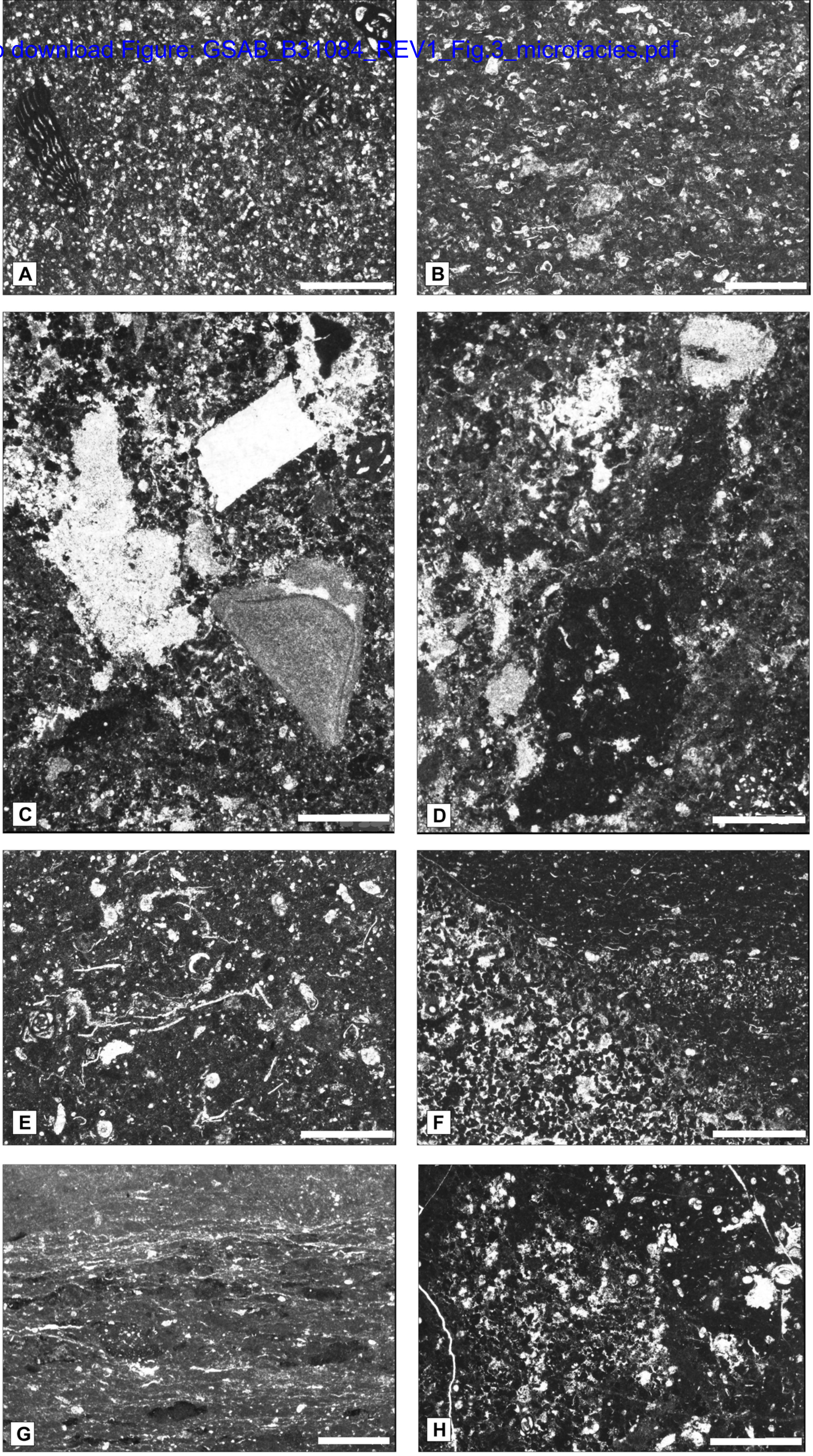

Figure 5
Click here to download Figure: GSAB_B31084R2_Fig.5-plankton.pdf

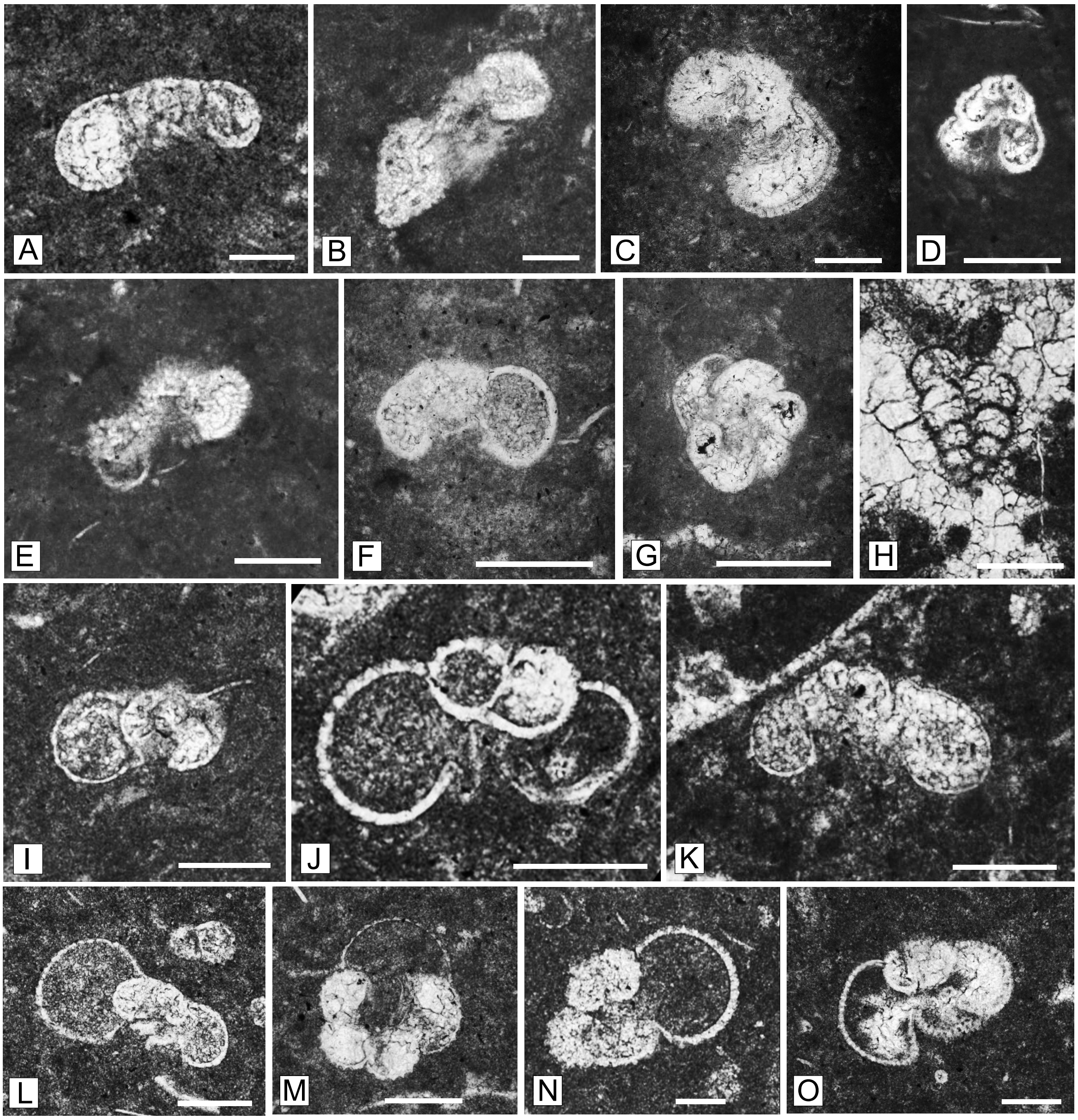

Figure 6
Click here to download Figure: GSAB_B31084R2_Fig.6-PGE norm.pdf

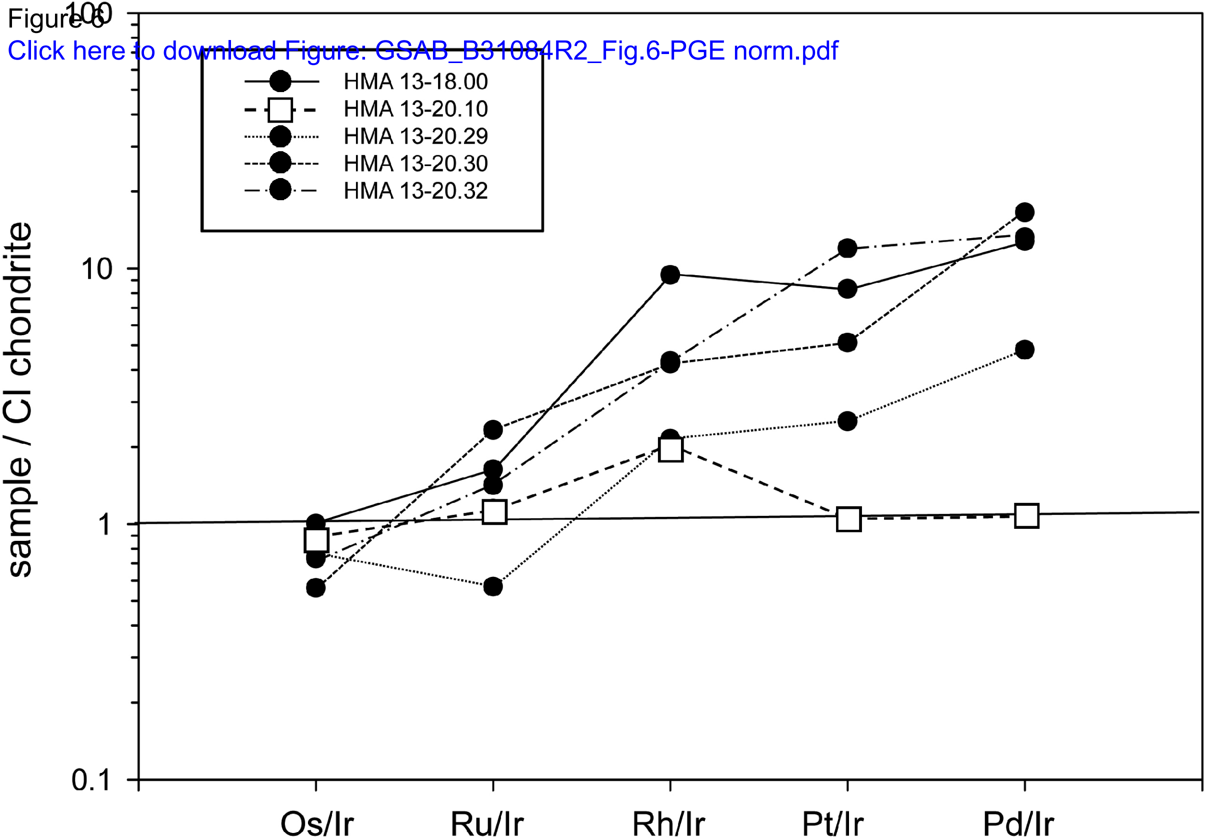

Figure 7
Click here to download Figure: GSAB_B31084_REV1_Fig.6 Atlantic_Tethys_2.pdf

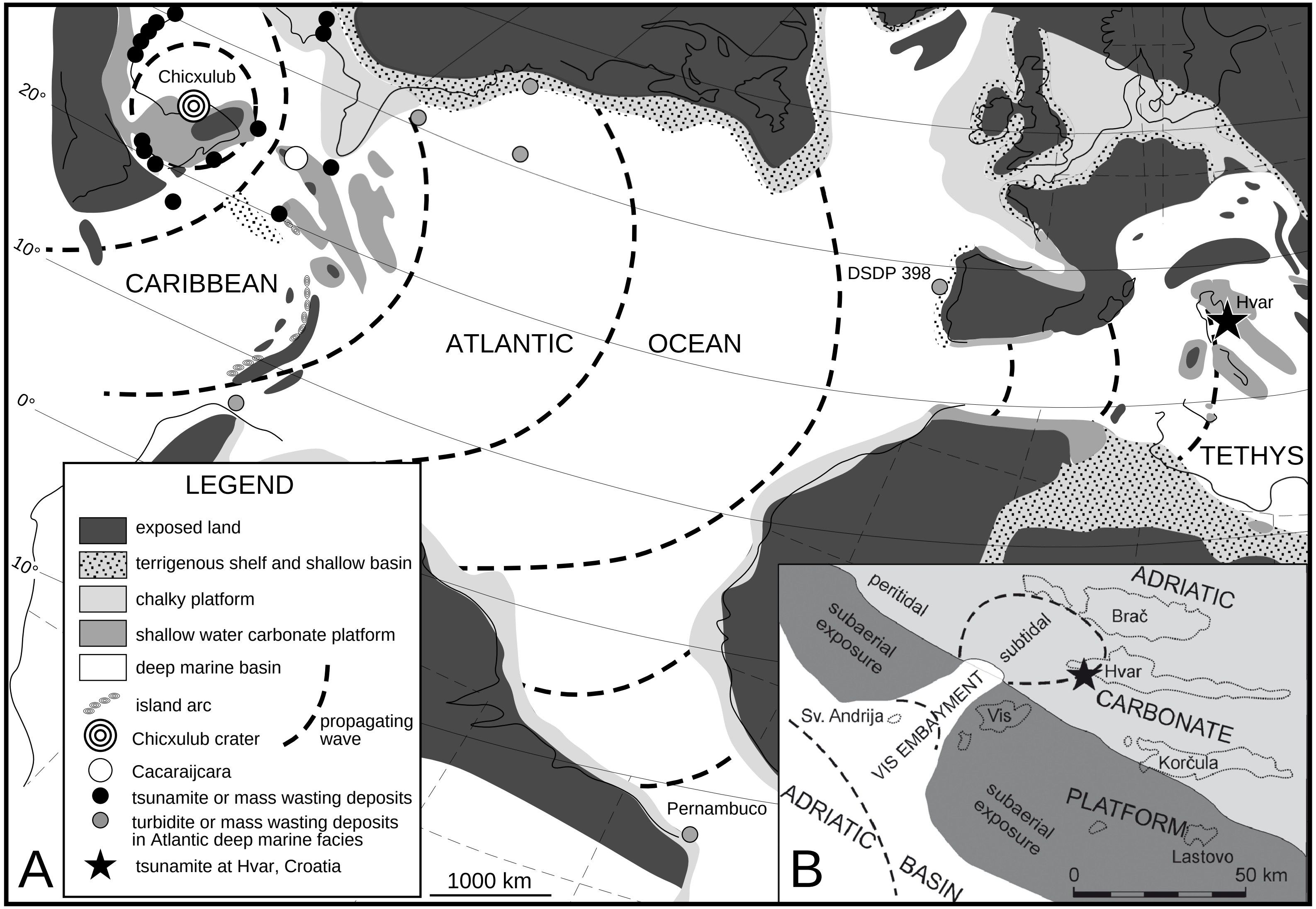

Fig. 6

Table 1

TABLE 1. STRONTIUM ISOTOPE STRATIGRAPHY OF THE MAJEROVICA SECTION

Sample	$^{87}Sr/^{86}Sr$	±2σ x10^{-6}	Sr μg/g	Mg μg/g	Fe μγ/g	Mn μg/g	$^{87}Sr/^{86}Sr$ mean	±2σ x10^{-6}	Age range
HMA-1							**0.707846**	**7**	**66.0-66.4**
HMA-1/1	0.707849	7	1069.0	1352	bdl	bdl			
HMA-1/2	0.707843	7	7955.7	1720	6.637	1.337			
HMA-1/3	0.707845	7	1080.0	1832	bdl	bdl			
HMA-2							**0.707850**	**7**	**66.0-66.5**
HMA-2/1	0.707842	7	1097.0	1343	2.628	bdl			
HMA-2/2	0.707860	7	940.3	1398	bdl	1.352			
HMA-2/3	0.707849	7	1070.0	1111	bdl	bdl			

Note: Samples are stored at the Croatian Geological Survey in Zagreb; All samples are from low-Mg calcite of rudist shells from Hvar-Majerovica (HMA) section (see Fig. 2B); Numerical ages are from Howarth and McArthur (1997, version 3:10/99, McArthur et al., 2001) corrected for the GeologicalTimeScale 2012, which places the K-Pg boundary at 66.04 ± 0.05 Ma; bdl = below detection limit.

Table 2

TABLE 2. ABUNDANCES OF PGE AND GOLD FROM THE K-Pg LIMESTONES OF THE MAJEROVICA SECTION

Sample	m level	Os ppb	Ir ppb	Ru ppb	Rh ppb	Pt ppb	Pd ppb	Au ppb
HMA13-15.30	15.30	0.05	0.06	0.30	0.08	1.58	0.87	0.82
HMA13-15.40	15.40	0.05	0.11	0.38	0.13	1.22	1.62	0.99
HMA13-18.00	18.00	0.06	0.06	0.15	0.17	1.09	0.98	0.80
HMA13-20.10A	20.10	0.41	0.59	1.00	0.27	1.33	1.01	0.63
HMA13-20.10B	20.10	0.47	0.51	0.97	0.32	1.63	0.69	0.43
HMA13-20.29A	20.29	0.13	0.16	0.14	0.10	0.72	0.88	1.25
HMA13-20.29B	20.29	0.12	0.19	0.21	0.12	1.03	1.15	1.29
HMA13-20.30A	20.30	0.08	0.14	0.29	0.12	1.51	1.59	0.54
HMA13-20.30B	20.30	0.11	0.11	0.38	0.15	1.12	2.32	0.63
HMA13-20.32A	20.32	0.08	0.11	0.23	0.14	2.08	1.85	0.32
HMA13-20.32B	20.32	0.11	0.09	0.18	0.09	2.40	0.76	0.17
HMA13-20.80	20.80	0.07	0.09	0.14	0.08	0.93	0.47	0.02
HMA13-25.60A	25.60	0.04	0.03	0.12	0.08	0.76	0.34	0.59
HMA13-25.26B	25.60	0.06	0.03	0.07	0.10	0.99	0.65	0.53
Standards								
WITS-1		1.38	1.45	4.07	1.12	7.07	5.59	6.11
TDB1		0.10	0.08	0.22	0.45	5.09	24.1	6.30
WPR1		12.3	14.1	21.7	13.6	298	233	39.9
Expected Values								
WITS-1 (1)		1.5	1.4 ± 0.3	3.9 ± 0.8	1.1 ± 0.2	5.7 ± 1.6	5.0 ± 1.2	1.4 ± 0.3
WITS-1 (2)		1.23	1.58	4.41	1.20	8.8	5.64	No data
TDB1 (2)		0.117	0.075	0.198	0.47	5.01	24.3	No data
TDB1 (3)		no data	0.15	0.3	0.7	5.8	22.4	6.3
WPR1 (3)		13	13.5	22	13.4	285	235	42

Note: Analyses carried out by NiS fire assay with ICP-MS see method description). Suffixes A and B refer to splits of crushed chips from the same sample. These were crushed to powder and analysed separately. Heterogeneity in these cases is expected to be worse than if they were true duplicates from the same volume of crushed powder. Sources for expected values as follows (1) Tredoux and McDonald, 1996; (2) Meisel and Moser, 2004; and (3) Govindaraju, 1994.

Table 3

TABLE 3: OSMIUM AND RHENIUM ISOTOPES FROM K-Pg LIMESTONES OF THE MAJEROVICA SECTION

Sample	$^{187}Os/^{188}Os$	Os (ppb)	Re (ppb)	Re/Os	$^{187}Re/^{188}Os$	$^{187}Os/^{188}Os$ (t)
HMA13-15.30	6.72 (2)	0.217	4.13	19.0	169.4	6.53 (2)
HMA13-15.40	6.57 (9)	0.253	15.42	61.6	541.9	5.92 (9)
HMA13-18.00	5.55 (2)	0.184	3.00	16.3	133.6	5.40 (2)
HMA13-20.10A	6.79 (3)	0.373	2.76	7.4	66.3	6.72 (3)
HMA13-20.10B	6.07 (1)	0.307	2.57	8.4	71.3	5.99 (1)
HMA13-20.29A	6.43 (4)	0.571	35.4	62.0	541.1	5.81 (4)
HMA13-20.30A	6.68 (4)	n.d.	9.91	-	-	-
HMA13A-20.80	5.49 (8)	0.312	4.70	15.1	122.8	5.36 (8)

Note: Initial $^{187}Os/^{188}Os$ ratios were calculated given the ^{187}Re decay constant (1.666 x 10-11 yr-1) from Smoliar et al. (1996), and an age of 65.5 Myr for the K-Pg boundary (Schulte et al., 2010, and references therein). The highly radiogenic initial $^{187}Os/^{188}Os$ ratios point towards enhanced crustal input into the marine environment from which these rocks formed, masking any possible small meteoritic signals. Rhenium concentrations most likely provide evidence for enrichments in an anoxic milieu.